

Estimating bridge criticality due to extreme traffic loads in highway networks

Mendoza Lugo, Miguel Angel; Nogal, Maria ; Morales-Nápoles, Oswaldo

DOI

[10.1016/j.engstruct.2023.117172](https://doi.org/10.1016/j.engstruct.2023.117172)

Publication date

2024

Document Version

Final published version

Published in

Engineering Structures

Citation (APA)

Mendoza Lugo, M. A., Nogal, M., & Morales-Nápoles, O. (2024). Estimating bridge criticality due to extreme traffic loads in highway networks. *Engineering Structures*, 300, Article 117172. <https://doi.org/10.1016/j.engstruct.2023.117172>

Important note

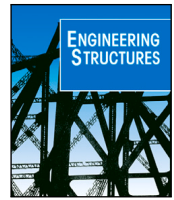
To cite this publication, please use the final published version (if applicable). Please check the document version above.

Copyright

Other than for strictly personal use, it is not permitted to download, forward or distribute the text or part of it, without the consent of the author(s) and/or copyright holder(s), unless the work is under an open content license such as Creative Commons.

Takedown policy

Please contact us and provide details if you believe this document breaches copyrights. We will remove access to the work immediately and investigate your claim.



Estimating bridge criticality due to extreme traffic loads in highway networks

Miguel Angel Mendoza-Lugo^{*}, Maria Nogal¹, Oswaldo Morales-Nápoles¹

Stevinweg 1, 2628CN Delft, The Netherlands

ARTICLE INFO

Keywords:

Bayesian Network
Copulas
Extreme value
Bridge network
Maps
Traffic load effects
Bridge criticality

ABSTRACT

Around the world, an increasing amount of bridge infrastructure is ageing. The resources involved in the reassessment of existing assets often exceed available resources and many bridges lack a minimum structural assessment. Therefore, there is a need for comprehensive and quantitative approaches to assess all the assets in the bridge network to reduce the risk of collapsing, damage to infrastructure, and economic losses. This paper proposes a methodology to quantify the structural criticality of bridges at a network level. To accomplish this, long-run site-specific simulations are conducted using Bayesian Networks and bivariate copulas, utilizing recorded traffic data obtained from permanent counting stations. To enhance the dataset, information from Weigh-in-Motion systems from different regions was integrated through a matching process. Subsequently, the structural response resulting from the simulated traffic is assessed, and the extreme values of the traffic load effects are obtained for selected return periods. Site-specific bridge criticality as a performance indicator for traffic load effects is derived by comparing the extreme load effects with the design load effects. The outcomes are mapped to facilitate visualization employing an open-source geographic information system application. To illustrate the application of the methodology, a total of 576 bridges within a national highway network are investigated, and a comparison with a popular simplified method is shown. The methodology herein presented can be used to assist in assessing the condition of a bridge network and prioritizing maintenance and repair activities by identifying potential bridges subjected to major load stress.

1. Introduction

The backbone of any country's transportation system is its national highway networks. They are essential to ensure the mobility of people and goods, thus driving economic growth. One of their most important assets is their bridge structures stock, when bridges are not properly used or maintained, perturbations take place in the traffic network. These perturbations generate a certain stress level in the network, leading to an increase in travel costs that can lead to greater economic losses [1]. Therefore, bridge management systems (BMS) are employed to control the bridge stock and provide data on the structural performance of bridges. A typical BMS consists of four modules, the Inventory Module, the Inspection Module, the Maintenance, Repair and Rehabilitation Module, and the Optimization Module [2]. In many countries, their BMSs are limited to the inventory module (single-module BMS). As a result, these BMSs are rarely used to make decisions regarding the risk and reliability of the bridge stock.

Bridge infrastructure is becoming old and outdated across the globe, for example, in the American continent, bridge inventories have shown that most bridges were constructed between 1960 and 1980 [3,4]. On the other hand, the majority of bridges in Europe were built

between 1970 and 2001 [5]. Deficiencies in past structural design, structural deterioration, and increasing traffic volume reveal the necessity for a structural reassessment of the existing bridge infrastructure to cope with ageing infrastructure. Vehicle loads monitoring is essential for maintaining bridge conditions. The data obtained from Weigh-in-Motion Systems (WIM) is essential for many applications such as the calculation of bridge performance indicators [6,7]. To compute these performance indicators based on traffic load monitoring, the primary step involves determining the load effects caused by the current traffic conditions. Much work has been done on modelling bridge loading due to traffic loads, [8–11] to name a few. However, most of the previous work is based on the assumption of the full availability of traffic data obtained with WIM systems and the complete bridge geometric and materials properties information. Additionally, these studies are focused only on one particular bridge or a set of few bridges with different span lengths. Such studies are the basis when the bridge design code needs to be calibrated, as the estimation of the characteristic values of the load effects of an entire bridge network is not feasible in most cases [8].

Numerous bridges lack a minimum structural assessment, which should include processes such as visual inspection, site-specific traffic

^{*} Correspondence to: Delft University of Technology, Department of Hydraulic Engineering, The Netherlands.

E-mail addresses: m.a.mendozalugo@tudelft.nl (M.A. Mendoza-Lugo), m.nogal@tudelft.nl (M. Nogal), o.moralesnapoles@tudelft.nl (O. Morales-Nápoles).

¹ Delft University of Technology, Department of Materials, Mechanics, Management & Design.

assessment, basic numerical models, examination of structural materials, and documentation review. This assessment serves to identify early concerns and maintenance needs, allowing bridge owners to prioritize further interventions based on the findings. Therefore, for bridge management the reassessment of the entire network is necessary. Information regarding the deterioration state of bridges and their structural behaviour over time are critical elements for bridge management on a network scale [12,13]. For example, recent studies in bridge maintenance strategies, use deep reinforcement learning (DRL)-based methods [14–16]. The DRL approach facilitates the selection of improved bridge maintenance strategies through interactive processes. It can be adjusted to obtain various performance metrics [17]. The inclusion of traffic loads can serve as one of the input parameters for DRL approaches.

Analysing traffic load effects on bridges, particularly the extreme values of the load effects (ELEs) is essential to assess the influence of heavy traffic on bridges. ELEs represent the maximum forces, usually bending moments and shear forces, experienced by a bridge during its lifetime. This analysis is crucial for ensuring the safety and reliability of infrastructure design and maintenance. Various probabilistic methods have been developed for this purpose, for example in [18] a methodology of extrapolating maximum load effects based on the level-crossing theory was introduced, [19] presents a Bayesian framework for predicting non-stationary bridge maximum traffic load effects and [20] proposes a clustering algorithm based on the generalized extreme value mixture model for data classification and extreme value extrapolation. However, the most common methods to estimate traffic ELEs include (i) fitting the Rice formula to the level-crossing rate of traffic load effects and extrapolating the load effects under the assumption of a stationary Gaussian process [21,22]; (ii) the peak-over-threshold method. In which the data above the threshold is fitted to the Generalized Pareto distribution [23,24], and (iii) the block maxima method in which the load effect due to each vehicle is computed and the maximum values of the selected block of time (usually one day) are selected and fitted to one of the three extreme value (EV) distributions, i.e., Gumbel, Weibull, and Frechet. The reader is referred to [25] for a complete overview of the techniques to estimate extreme load effects on bridges.

On the other hand, one of the most popular simple methods of computing ELEs on two-lane bridges is the (extended) Turkstra's Rule [26, 27]. According to this rule, the N -year loading event, where N could be any return period in years, is generated when the N -year truck encounters a more frequent truck, such as the one-month or one-week truck. Another variation of Turkstra's rule, as reported by [28], suggests that for bridges with high lateral distribution, the critical loading event for bending moment involves a very heavy vehicle, 60% to 80% of 1000-year Gross Vehicle Weight (GVW), in the slow lane and a moderately heavy vehicle (50 to 60 tons) in the fast lane. In the case of shear at the supports, the dominant event type is usually a single extremely heavy truck in the slow lane, 75% to 95% of the 1000-year GVW. Despite its accuracy in specific scenarios, Turkstra's Rule has shown significant inaccuracies in other cases [29,30].

Two main problems exist when studying the effects of traffic loads on bridges at a network scale. (i) In many locations, WIM systems are not a viable option due to their elevated costs. Traditional traffic counters are the option when a large volume of traffic data is needed. The disadvantage of these devices is that axle loads are typically not measured. (ii) Bridge inventories usually lack detailed information regarding the geometric and material properties of the bridges. Typically, the information contained in the inventories is the number of spans, the length of the bridge, and its width. Specific information on cross-section, material strengths, and steel reinforcement is rarely recorded. These two problems highlight the need for approaches and methodologies that can overcome the limitations imposed by cost constraints and insufficient inventory information. Furthermore, when large-scale studies are needed, maps are needed because of their ability to present summarized information that can be required in the decision-making

process. Different engineering fields such as hydraulic, wind, seismic, and transport engineering [31–34] have used maps as a useful tool for hazard modelling. However, to the best of the authors' knowledge, maps of ELEs or load effects performance indicators of a bridge network do not exist in the scientific literature.

In this paper, we introduce a valuable methodology that allows mapping and estimating the extreme load effects due to heavy vehicle (HV) traffic. Our main objective is to evaluate the structural effect of actual traffic loads in comparison to its effect under the design live load model provided by the bridge owner. This comparison serves as a means to assess the criticality of bridges as performance indicators for traffic load effects at the network level. We take into consideration the specific traffic configuration at each site and the limited information available on single-module BMSs. This is of relevance for bridge maintenance strategies since it can help the development of strategies to prioritize maintenance, especially in locations or bridge networks in which WIM systems are not the main source of traffic data. The development of the methodology had a dual purpose: (a) to perform a large-scale simulation of site-specific truck traffic and compute its effects on corresponding bridges and (b) to estimate the ELEs of an entire bridge network and perform spatial analysis using geographic information system (GIS) software. The methodology consists of four tasks: site-specific traffic simulation, numerical modelling and analysis of bridge structures, extreme value analysis for ELEs, and bridge criticality computation. To achieve these objectives, this paper proposes a simple method that uses Gaussian copula-based Bayesian Networks to simulate site-specific synthetic observations of HVs, copulas to characterize inter-vehicle gaps that will simulate traffic flow and extreme value theory to estimate ELEs. The methodology presents various favourable attributes, such as the capability to identify bridges that require more detailed inspections due to their condition as assessed by the model, a simple conceptualization that is easy to apply and requires only basic information regarding traffic and bridge characteristics, the flexibility to be applied to any bridge network, and the ability to help create a more robust single-module BMS.

To illustrate the use of the methodology, the national bridge network of Mexico is selected. Mexico's national bridge network is a clear example in which there is no WIM information available and is bounded to a single-module BMS. Therefore, the results of the applied methodology will allow for easily identifying bridges in need of inspection given the limited information available. The remaining document is organized as follows. In Section 2 the methodology together with the bridge network case study is presented. The application of the method for one particular bridge is shown in Section 3. The results regarding all bridges on the example network, and the comparison with the simplified Turkstra's Rule method are given in Section 4. Finally, in Section 5, the conclusions are drawn.

2. Methodology to estimate extreme load effects and bridge criticality

The aim of this research is to determine and map the extreme load effects and the bridge criticality arising from traffic loads across a bridge network, where data obtained from WIM systems is not the principal source. In order to carry out this extensive task, we present a simple methodology, shown in Fig. 1, that can be summarized into four main tasks. (i) Site-specific traffic simulation; statistically representative synthetic traffic is simulated based on real traffic data from the study sites by modelling correlations between the variables of interest (axle loads, inter-axle distances, and inter-vehicle gaps). This step leverages previous research (see [35–37]). (ii) Numerical modelling and analysis of the bridge structures; selected load effects time histories of the bridges under study are computed by applying the synthetic traffic to a numerical model of the structures. (iii) Extreme value analysis for extreme load effects; statistical analysis of load effects time histories by extreme value theory is carried out to characterize extreme events with

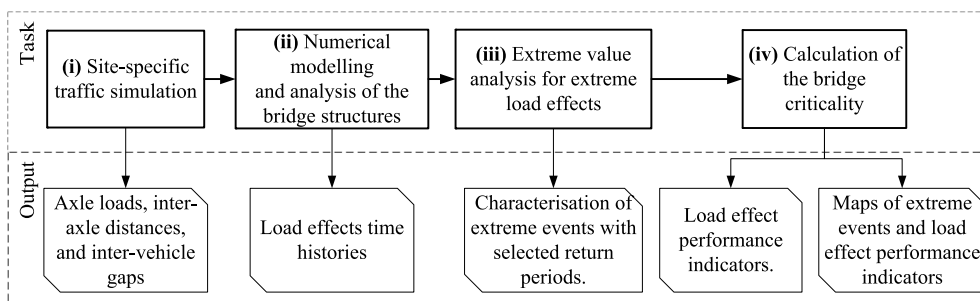


Fig. 1. Framework estimating extreme load effects and bridge criticality.

selected return periods. (iv) Calculation of the bridge criticality; load effect performance indicators are derived by comparing the extreme load effects with the design load effects. In addition, the computed extreme events and bridge criticality are mapped to visually identified changes, trends, and hot spots that may require attention and support in the design and implementation of maintenance strategies.

This study is conducted using open-source tools. The analysis is done through Python programming language, extensively used nowadays. The Python libraries used in this work (in addition to the main libraries such as NumPy, pandas and SciPy) are PyBanshee [38] and pyvinecopulib [39] for traffic simulation, PyNite [40] for the computation of the load effects on bridges and Geopandas [41] to work with the geospatial data. The outcome maps are implemented using QGIS v3.10 [42], a free and open-source cross-platform desktop geographic information system (GIS) application. To enhance clarity and ease the introduction of the methodology, the four tasks will be described in the following sections, using the case study as a context.

2.1. Case study: Major highway corridors bridge network of Mexico

The most important elements of the national road network of Mexico are the toll-free fifteen major highway corridors (MHC) which extend over 20000 km approximately and account for over 55% of the country's highway traffic flow. The toll-free MHC network is managed by the Ministry of Communications and Transportation (SCT, for its acronym in Spanish).

2.1.1. Mexican bridge system

Mexico has a system for bridge management, conservation, and maintenance called the Mexican Bridges System (SIPUMEX, for its acronym in Spanish). This system logs the structural state of individual assets in order to program maintenance work. The SIPUMEX database [43], provides general information, such as the name of the bridge, construction date, total bridge length, number of spans, material, and type of structure. Concerning traffic data, the database provides design load, annual average daily traffic (AADT), the vehicle types and the vehicle type distribution that constitutes the traffic flow per bridge. However, the only reported vehicle types are trucks, buses and normal passenger cars and no further specification is presented.

For the purpose of this investigation, we applied the filter criteria shown in Table 1. These criteria have been selected to align with the objectives of the presented study. Firstly, we included bridges situated on the fifteen MHCs under examination (filter 1). Secondly, according to SCT standards [44], a bridge is defined as having a minimum span length of 6 meters (filter 2). Furthermore, the study focuses on heavy traffic loads, hence only road bridges are considered (filter 3). This criterion aligns with SCT standards, which stipulate a minimum carriage width of 4 meters for road bridges (filter 4) [44]. It is important to note that SCT manages only Overpass bridges (filter 5). To simplify the structural analysis, we considered only non-horizontal curved, non-skewed, and concrete bridges (filters 6, 7, 8). Additionally, the methodology used to estimate bridge criticality requires bridges with

Table 1
Filter criteria to select the bridges under study.

Filter no.	Criteria	Number of bridges remained after the filter	Number of filtered bridges
1	Bridges located at the 15 MHC	1776	5828
2	Minimum span length of 6 m	1552	224
3	Road bridges	1416	136
4	Minimum carriageway width of 4 m	1390	26
5	Overpass bridges (PSV for its acronym in Spanish)	1317	73
6	Non-horizontally curved bridges	1222	95
7	Non-skew bridges	801	421
8	Concrete bridges	695	106
9	Bridges with reported design live load	675	20
10	The sum of span lengths should be equal to the total bridge length	576	99

reported design live loads (filter 9). Finally, the inclusion of the span length criterion was intended to eliminate any erroneous measurements or inconsistencies within the dataset (filter 10). As a result, 576 bridges remained, hereafter referred to as the major highway corridors bridge database (MHCB).

Fig. 2 shows a general statistical characterization of the MHCB database. Regarding the age of the structures, around 65% of the bridges (376 bridges) are 50 years old or more, most of them constructed in 1960 (older than 60 years, see Fig. 2a). The most frequent max span length is 6.6 m (Fig. 2b). Similarly, most of the bridges have a carriage width of 7 m (two lanes, Fig. 2c). Approximately, 50% of the bridge structures are single-span systems, while the other structures consist of multi-span bridges with up to seventeen spans, out of which 28 are continuous bridges (Fig. 2d). As can be seen in Fig. 2e around 67% of the bridges (387 bridges) were originally designed for load model HS15-44 (three-axle AASHTO standard HS truck with a gross vehicle weight (GVW) of 24.5 t approximately [45]) or HS20-44 (three-axle AASHTO standard HS truck with GVW \approx 32.6 t [45]). The remaining were designed for the Mexican vehicles T3S3 (three-axle truck plus three-axle semitrailer) and T3S2R4 (three-axle truck plus two-axle semitrailer plus four-axle trailer). Regarding the condition of the bridges, 234 structures (41%) have a 2 or 1 rating which corresponds to bridges with minor problems and bridges in good condition (see Fig. 2f).

2.1.2. Traffic data

As mentioned in Section 2.1.1, information regarding traffic in the SIPUMEX database is limited. Additionally, the use of WIM systems in Mexico is very scarce [46,47]. Nevertheless, in an effort to know the yearly traffic trends on the Mexican highway network, the SCT installed a set of automatic vehicle counters and survey stations in key locations. As a result, the Mexican authorities publish the two most important traffic data sources in Mexico: the road data (*Datos viales*

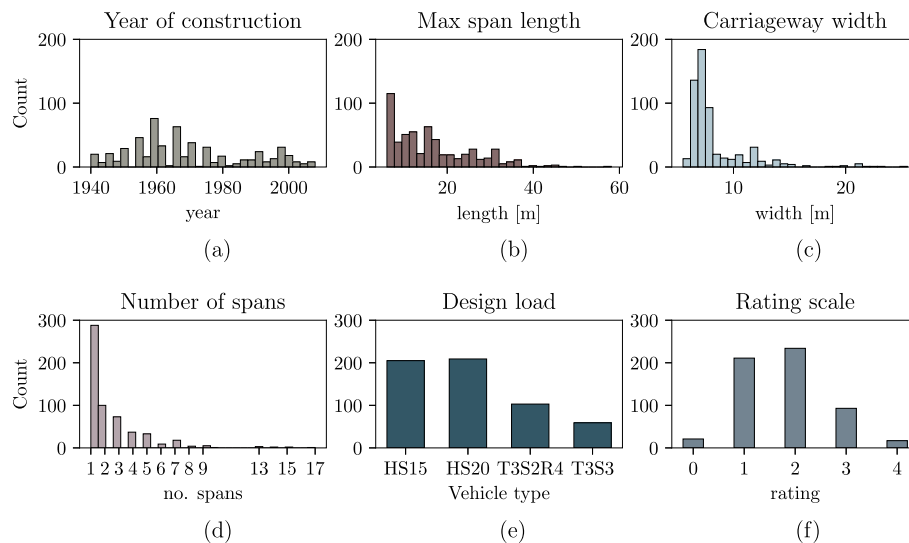


Fig. 2. General statistical characterization of the bridges under study. (a) Year: Max = 2008, Min = 1940, Mode = 1960. (b) Length[m]: Max = 58.1, Min = 6.0, Mode = 6.6. (c) Width[m]: Max = 25.5, Min = 5.5, Mode = 7.0. (d) No. spans: Max = 17, Min = 1, Mode = 1. (e) Vehicle type: Mode = HS20. (f) Rating: Max = 4, Min = 0, Mode = 2.

in Spanish) database [48] and the statistic field study of domestic road transportation (EECAN, for its acronym in Spanish) database [49].

The *Datos viales* database is published by the Department of Infrastructure. The last publicly available database (*Datos viales* 2021) has information on more than 11 000 counting stations. It contains information such as the name of the road, the name of the counting station, the lane direction, the annual average daily traffic (AADT), and the proportion of vehicle types that conform to the traffic flow. The vehicle types presented in the database are motorcycles (M), automobiles (A), buses (B), single unit vehicles with two or three axles (C2, C3), three-axle truck plus two-axle semitrailer (T3S2), three-axle truck plus three-axle semitrailer (T3S3) and three-axle truck plus two-axle semitrailer plus four-axle trailer (T3S2R4) and “others” (Otros). However, it does not provide information regarding gross vehicle weight, individual axle loads, or inter axle distances, necessary parameters for the computation of extreme load effects on bridges [50].

The second major traffic source, the EECAN database, is a compilation of data on vehicles passing through origin–destination survey stations installed on the road network administered by the federal government [51]. The origin–destination surveys have been conducted each year, from 1991 to 2017, by the SCT. In terms of vehicle attributes, the EECAN database provides the information needed to simulate and estimate the extreme load effects on bridges, such as vehicle type, gross vehicle weight and individual axle loads. The EECAN database is publicly available on the website of the Mexican Transport Institute. Data from 233 survey stations (from 2002 until 2017) include information from about 1.3 million surveyed vehicles of which, vehicle types C2, C3, T3S2, T3S3 and T3S2R4 are the most common HVs, those with $GVW \geq 34$ kN [52], reported. The vehicle classification is done according to their class, nomenclature (code) and the number of axles in [52]. The visual representation (silhouette), vehicle code (i th vehicle type) and its corresponding number of axles (n_i) of the most common HVs are presented in Table 2. For more details, the reader is referred to [48,51].

2.2. Site-specific traffic simulation

In order to generate accurate synthetic traffic data statistically representative of the real observations, statistical correlations between the variables of interest need to be modelled. Previous studies such as [23,53,54], have simulated traffic data using empirical factors, linear correlations, and copulas. These studies focus only on axle loads, some

provide fixed inter-axle distances and in most of them, the correlation between axle loads is not taken into account. However, we are interested in modelling GVW, individual axle loads, inter-axle distances and inter-vehicle gaps. With this aim, we use the Bayesian Network approach presented in [37] which is based on previous studies such as [55–57] and recently used in [58]. This approach is explained in the following sections.






2.2.1. Synthetic heavy vehicles

Bayesian Networks are directed acyclic graphs that represent a set of random variables in their nodes and (un)conditional dependencies between the variables in their arcs [59]. One type of BN that has the advantage of managing efficiently hundreds of variables is the Gaussian copula-based Bayesian network (GCBN) [60]. We use the GCBN model GCBN_{EECAN} developed by [37]. As the name of the model suggests, GCBN_{EECAN} allows the generation of synthetic axle load observations similar to those reported in the EECAN database. The model, originally quantified with over 750 000 HVs, consists of 26 nodes representing individual axle loads of the five HVs presented in Table 2 and 45 arcs corresponding to the (un)conditional rank correlations between axle loads. The output of the GCBN model is a database (different every time that the model runs) that contains the variables: vehicle type, gross vehicle weight and individual axle loads. Fig. 3 shows the Gaussian copula-based Bayesian Network model employed for this work.

One of the limitations of the GCBN_{EECAN} model is that inter-axle distances and inter-vehicle gaps are not modelled, as information on these variables is not recorded in the EECAN database or in other available Mexican traffic sources. The most reliable technology that delivers loads and wheelbases (inter-axle distances) is WIM, unfortunately, as mentioned in Section 2.1.2, the use of WIM systems in Mexico is very scarce, and publicly available WIM data is non-existent. To complement the missing data we used information from a Dutch WIM database. WIM traffic observations taken on highways A12 (kilometer point, KP, 42) Woerden, A15 (KP 92) Gorinchem and A16 (KP 41) Gravendeel in April 2013 constitute the database. It includes information on more than 150 000 HVs grouped into more than 200 vehicle classes according to their WIM codes. This database has been employed in several studies such as [35,56,61,62].

For a complete overview and details regarding the accuracy of the GCBN model GCBN_{EECAN}, the reader is referred to the original source [37]. In this source, EECAN measurements are discussed, including the application of filtering criteria to ensure data quality and the utilization of Gaussian Mixture distributions to model individual

Table 2
Main heavy vehicle types with $GVW \geq 34$ kN found in ECCAN database.

Silhouette	Vehicle (i)	Type (code)	No. axles (n_i)
	1	C2	2
	2	C3	3
	3	T3S2	5
	4	T3S3	6
	5	T3S2R4	9

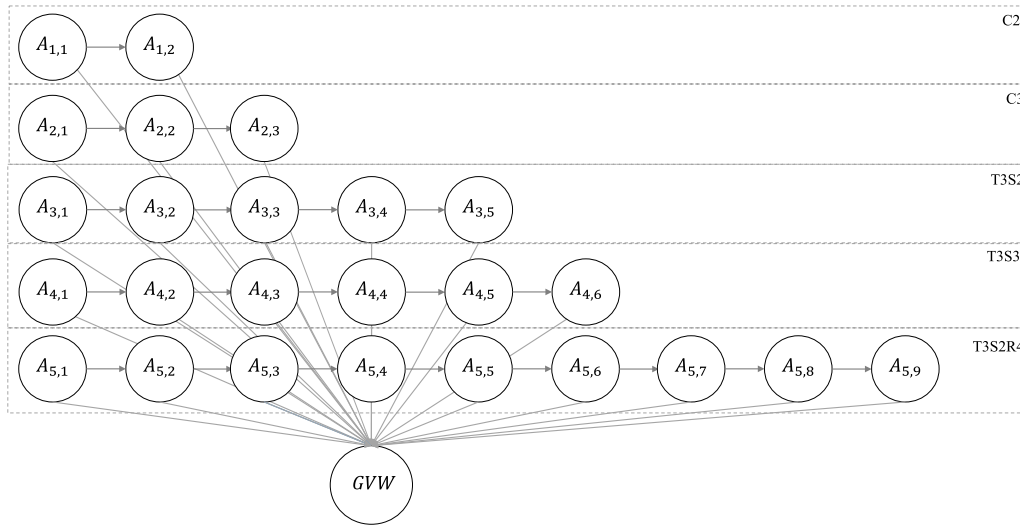


Fig. 3. Gaussian copula-based Bayesian Network $GCBN_{ECCAN}$. Each row of nodes represents one of the five vehicle types illustrated in Table 2. $A_{i,j}$ denotes a random variable representing the j th axle load of the vehicle type i . GVW is the random variable gross vehicle weight regardless of vehicle type. The arcs correspond to the (un)conditional rank correlations between individual axle loads per vehicle type.

axle loads to deal with the uncertainty of the measurements. Similarly, for detailed information regarding specific details and the modelling of dependence and uncertainty in the Dutch WIM database, the reader is referred to [35].

As the SCT report [63] provides the only reliable source of inter-axle distances for the five main Mexican heavy vehicles, we matched the Dutch and Mexican vehicles based on the number of axles, number of consecutive axles, and body configuration. The consecutive axles are defined as those with centre distances ranging from 100 cm to 243 cm apart, as specified in previous literature [52,64]. For example, the Mexican vehicle T3S2 will correspond to the Dutch WIM code T1202. For each matched vehicle, we selected inter-axle distance samples from the WIM data, which exhibited similar mean and coefficient of variation as reported in [63]. Then, the Pearson correlation between inter-axle distances of the matched vehicles is calculated and the resulting values are stored. We created five empirical GCBNs, one for each vehicle type, to generate synthetic samples of inter-axle distances. As an example, Fig. 4 shows the GCBN for vehicle type T3S2, which consists of five nodes representing individual inter-axle distances and four arcs corresponding to the (un)conditional rank correlations between inter-axle distances. For each group of axle loads of a particular vehicle type generated with the $GCBN_{ECCAN}$ model, the inter-axle distances are generated using the corresponding inter-axle distance GCBN. Table A.1 presents a comparison between the general statistics mean and coefficient of variation between the synthetic inter-axle distances and the reported in the SCT study. A similar approach used for axle space modelling is described in [35].

2.2.2. Inter-vehicle gaps using copulas

The distance between vehicles (gaps) has been studied by many researchers. Some used standard free-flow models by modelling the



Fig. 4. T3S2 Inter-axle distances GCBN. $D_{i,j}$ denotes a random variable representing the j th inter-axle distance of the vehicle type i ($i = 3$ correspond to vehicle type T3S2). $D_{i,1}$ is the distance between the front of the vehicle and the first axle, $D_{i,2}$ is the distance of the first axle to the second, and so on. The arcs correspond to the (un)conditional rank correlations between individual inter-axle distances.

distance between stationary vehicles with a beta distribution (for example see [8,65]). Others have used advanced techniques, such as traffic microsimulation based on Intelligent Driver Model [66], which is capable of modelling car following or lane changing [67,68]. These advanced techniques are needed when conducting detailed and local-scale bridge analyses, such as the performance of hinged joints [69]. On the other hand, when a global bridge assessment is conducted, standard free-flow models can serve to simulate the distance between vehicles and to indicate the transverse position with the lane where the vehicle is located [68].

For this work, a free-flow traffic pattern is assumed for all lanes of all bridges under study. This is because the traffic loading congestion effect is usually more characteristic of long-span bridges [70] and urban studies due to the complexity of the traffic network and abundant local detours [71]. In order to capture the dependence between gaps [28], a copula-based approach is used. The copula-based approach can characterize the random variable inter-vehicle gap by estimating its auto-correlation. This approach has been used in [55,57,58]. Copulas are joint distributions with uniform marginals in $[0,1]$. Any multivariate joint distribution can be written in terms of a copula that describes

the dependence between the random variables and their corresponding uni-variate marginal distribution functions [72]. For specific details regarding copula modelling the reader is referred to [73] and references therein.

Let Y denote a random variable representing the inter-vehicle gap with distribution F_Y . Since we are interested in the time series $\{Y_t\}$, $t \in \mathbb{N}$, the conditional distribution function of a bivariate copula $C_{\theta_Y}\{F(y_t), F(y_{t-1})\}$ is given by

$$H(y|y_{t-1}) = P(Y_t \leq y_t | Y_{t-1} = y_{t-1}) = C_{\theta_Y}(F(y_t)|F(y_{t-1})) \quad (1)$$

where $C_{\theta_Y}(F(y_t)|F(y_{t-1}))$ is the conditional copula and it would model the order 1 auto-correlation for the time series of interest. θ_Y are the parameters that summarize the dependence between $F(y_t)$ and $F(y_{t-1})$. To model the inter-vehicle gaps the following assumptions are made: (1) Only HVs are considered, (2) the distance from the HV's rear to the front of the subsequent HV is considered, (3) correlations between lanes are not taken into account, (4) due to the absence of reliable inter-vehicle gap data for Mexico, the Dutch WIM database from highway A12 (see Section 2.2.1) is used to model the inter-vehicle gaps and (5) only weekdays are considered. Hence, the vehicle gaps simulation algorithm can be summarized as follows:

- i Select only the weekdays of the month and group each day dataset by hours.
- ii Select the first weekday and the vehicle gaps observations of the first hour $F(y_t)$.
- iii Fit the suitable copula $C_{\theta_Y}\{F(y_t), F(y_{t-1})\}$.
- iv Repeat steps ii and iii for the remaining hours of the day and weekdays. Let $hr = \{1, 2, \dots, 24\}$ be a set representing hours of a day and $d = \{1, 2, \dots, 20\}$ the set that represent weekdays. Hence, for the study WIM dataset, 480 copulas $C_{\theta_Y}^{d,hr}\{F(y_t), F(y_{t-1})\}$ for one lane are quantified.
- v Simulate the desired vehicle gaps for the first hour using the conditional copula according to the best-fitted copula. Use as seed for the first value of the next hour and the last value of the previous hour.

In total, 960 (2 lanes \times 20 weekdays \times 24 h/day) copulas are quantified Bayesian information criterion [74] is used to select the best-fit copula. As an example, Table A.2 shows the copula fits of weekday $d = 7$ (9 of April 2013). The first column corresponds to the hour of the day. The 2nd column corresponds to the copula notation. Columns 3 and 4 to the name of and parameter of the copula correspondingly. The 5th column to Spearman's ρ rank correlation [75]. The last column corresponds to the percentage of the total HVs in one day per hour. Notice that for this particular case, stronger correlations can be found at the latest hours of the day and the traffic volume is mostly concentrated between 4:00 h and 18:00 h. Additionally, Fig. 5 shows 5 days of HV inter-vehicle gaps observations. Peaks occur at the end (or beginning) of each day since fewer HVs circulate in the early hours of the day. It is important to note that traffic densities, and consequently inter-vehicle gaps, are site-sensitive and can vary significantly based on the specific characteristics and conditions of each country's transportation network. However, for the purpose of demonstrating the methodology presented here and acknowledging the unique characteristics of the study network, it is pointed out that the traffic volume of HVs in the study network is lower compared to the Dutch highway A12 WIM location. Consequently, the results obtained from the analysis may be conservative.

2.2.3. Traffic simulation

In order to simulate site-specific HV traffic flow for each one of the 576 bridges in the MHCb, SIPUMEX, EECAN and *Datos Viales* are merged. First, by using QGIS neighbour analysis is conducted to find the nearest counting station to each bridge. The resulting output provides a map of the spatial distribution of the nearest counting stations (298

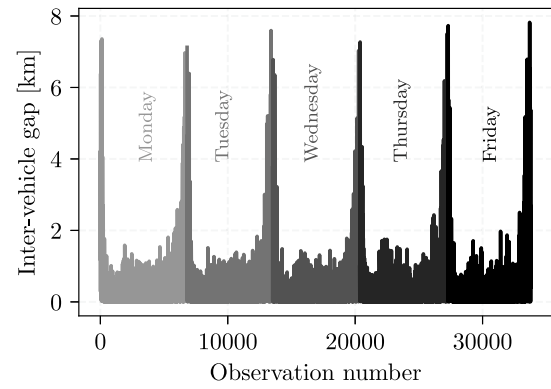


Fig. 5. Inter-vehicle gaps time series of observations measured in the WIM station A12 left lane corresponding to the days 8 to 12 of April 2013.

in total) to each of the bridges under study. The traffic information provided by the resulting counting stations is used to simulate the traffic passing by a particular bridge. It should be noted that the information regarding HV types in the three databases corresponds to the HV types presented in Table 2.

Let $\{b\} = \{1, 2, \dots, 576\}$ be a set of indices that correspond to the 576 bridges under study and $\{c\} = \{1, 2, \dots, 298\}$ a set of indices corresponding to the 298 counting stations. $K_c = \{1, 2, \dots, 5\}$ a set whose elements represent the number of total HV types registered in counting station c . H is a set whose elements represent the individual HV types presented in Table 2. The necessary input data to compute site-specific traffic for a bridge b are: (i) the number of HV types at the closest counting station of the study bridge b (K_c^b), (ii) the subset $I \subseteq H$, with K_c elements, registered in c (I_c^b), (iii) the proportion of the traffic flow per HV type $i \in I$ ($p_{c,i}^b$) and, (iv) the annual average daily truck traffic (AADTT $_c^b$). Therefore, a site-specific GCBN $_c^b$ model is quantified using only the K_c^b vehicle types registered in the counting station c travelling over bridge b , i.e., $GCBN_c^b = GCBN_{EECAN} \left(K_c^b; I_c^b; p_{c,i}^b; AADTT_c^b \right)$. We compute $N_c^b = \sum_{i=1}^{K_c^b} (AADTT_c^b \cdot p_{c,i}^b)$ un-conditional samples using the site-specific GCBN $_c^b$. The output of the model is the site-specific synthetic axle load observations for the bridge of interest. Finally, for each vehicle generated, inter-axle distances and inter-vehicle gaps are assigned as described in Section 2.2. The output database contains $k = 1, \dots, N_c^b$ HVs with the attributes: vehicle type, gross vehicle weight, individual axle loads, individual inter axle distances and the gaps between vehicle k and vehicle $k - 1$.

2.3. Numerical modelling and analysis of the bridge structures

In this work, two load effects are considered, i.e., the absolute bending moment (M in kN m) and the absolute shear force (V in kN). For computational efficiency purposes, the methodology to analyse the bridge structures and determine the load effects is based on the method of influence lines. This approach is a conventional engineering technique that employs influence lines to illustrate how a load effect, such as moment, shear force, reaction, or deflection, changes at a specific point or component of a structure as a concentrated loading action moves across the structure. In essence, an influence line visually depicts the variation of the load effect as the concentrated loading action traverses the structure [76,77].

To perform the structural analysis of the 576 bridges, the following assumptions are made: (1) the bridges are modelled as a series of interconnected beams, (2) the analysis is based on the principles of the Euler-Bernoulli beam theory, (3) to address the lateral distribution of loads, the weights of trucks travelling in the fast lane are adjusted using lane factors. Regarding bending moments, an equal contribution is considered from each lane, which is represented by a factor of 1. As

for shear force, a factor of 0.45 is applied based on the Refs. [28,78], (4) second-order effects are neglected, (5) dynamic effects due to moving loads are neglected and (6) independent streams of synthetic traffic are generated for each lane [78]. It is important to note that the numerical modelling to perform the structural analysis is based on the linear assumption. However, the design of a bridge is based on the non-linear assumption in order to capture more complex behaviour such as fatigue and buckling.

The procedure for computing the load effects is as follows. First, a grid is specified in each bridge with a grid size of 0.2 m, resulting in a total of $\lfloor L^b/0.2 \rfloor + 1$ individual positions along the structures, where L^b is the total length in m of the bridge b . The number of individual positions varies since each bridge has different lengths. A discrete unit load is applied on each position along the bridge to compute the resulting bending moments and shear forces cases. These results are gathered in two matrices \mathbf{U}_M^b and \mathbf{U}_V^b that represent the bending moments and the shear forces caused by the point load in each point on the grid along bridge b . By using the superposition principle, each resulting matrix is multiplied by the axle loads vector \mathbf{A} of each convoy of vehicles (or single vehicle). Hence, the axle loads can be acting in any of the grid points. For each situation, the unit matrices are multiplied by the value of the moving axle loads. Finally, the sum of the multiplication leads to the load effect for the particular convoy or single vehicle driving through bridge b ($\mathbf{M} = \mathbf{U}_M^b \cdot \mathbf{A}$ for example). The envelope of all load effects caused by each vehicle provides the maximum load effects.

2.4. Extreme value analysis for extreme load effects

Previous studies have provided an assessment of statistical approaches for evaluating load effects using different quantities of data (see for example [79–81]). One of the most comprehensive studies in this regard was conducted by [25]. In this study, seven statistical inference methods, including Peaks-Over-Threshold, Generalized Extreme Value (GEV), Box–Cox, Normal, Rice formula, Bayesian Inference, and Predictive Likelihood, were critically reviewed. The results of this study revealed that, among these seven methods, the approach of fitting block-maximum data to a GEV distribution is the most widely employed and accepted technique for analysing bridge traffic loading, typically using a one-day block size.

The block maxima approach has a drawback because it considers only one extreme event in each time block, potentially leading to the omission of significant data. On the other hand, this method offers numerous advantages for load effects analysis. It stands out as the default choice, appreciated for its practicality in capturing daily variations and versatility in handling various scenarios. The main advantage is the time referencing of the data, a crucial requirement when computing lifetime probabilities of exceedance, leading to effectiveness in estimating characteristic values in simple and complex scenarios. Consequently, extreme value analysis based on the block maxima method is used in this work to estimate the ELEs on the bridges under investigation.

Assuming that the block maxima load effects are independent, the block maxima is fitted to one of the extreme value distributions described in Eq. (2), which corresponds to the GEV distribution, where μ is the location parameter, σ is the scale parameter and ξ is the shape parameter. There are three types of extreme value distributions characterized by the parameter ξ . When the parameter ξ equals 0, the distribution is a Gumbel distribution, when ξ is greater than 0, it is a Fréchet, and when ξ is less than 0, it is a Weibull distribution [82]. As noted by [83], finite or bounded variables cannot have a maximal domain of attraction of Fréchet type. Given that the load effects cannot take infinite values, only Gumbel or Weibull distributions are possible [25]. Therefore, these two types of extreme value distributions are

considered.

$$F(x; \mu, \sigma, \xi) = \begin{cases} \exp\left(-\left(1 + \xi\left(\frac{x-\mu}{\sigma}\right)^{-\frac{1}{\xi}}\right)\right), & \text{if } \xi \neq 0 \\ \exp\left(-\exp\left(-\frac{x-\mu}{\sigma}\right)\right), & \text{if } \xi = 0 \end{cases} \quad (2)$$

For this work, the load effect data for each bridge are grouped into blocks of one day and the maximum value in each block is recorded (daily maxima). Maximum likelihood estimation is the preferred method for estimating the parameters that better describe the daily maxima data. In addition, to find the parameters and distributions, we choose to truncate the likelihood function [84]. This is done by selecting a truncated load effect value x_0 . The choice of x_0 is guided by two considerations: (i) the larger the truncated value, the better the found distribution will accurately describe the tail of the frequency distribution and (ii) the smaller the truncated load, the more data will be used in the part of the likelihood function that accounts for the tail. The data in $\mathbf{x} = \{x_1, x_2, \dots, x_n\}$ is rearranged so that: $\{x_1, \dots, x_l\} \leq x_0$ and $\{x_{l+1}, \dots, x_n\} > x_0$. The truncated-likelihood function of the sample \mathbf{x} can be written according to Eq. (3).

$$L_x(x; \mathbf{a}) = \{F_x(x_0; \mathbf{a})\}^l \prod_{h=l+1}^n f_x(x_h; \mathbf{a}) \quad (3)$$

where \mathbf{a} is the parameter vector of the distribution. The vector of parameters can be determined as usually by maximizing the logarithm of the likelihood. The first factor in the right-hand term of Eq. (3) ($\{F_x(x_0; \mathbf{a})\}^l$) means that for values smaller than x_0 , we only consider the probability that they are smaller or equal than x_0 . On the other hand, the second factor ($\prod_{h=l+1}^n f_x(x_h; \mathbf{a})$) means that for values greater or equal to x_0 , we take the usual approach to likelihood estimation using the probability density. This method is used, for example, in [85] and in [86] to advise the Dutch authorities regarding overloaded vehicles. Notice that it is equivalent to estimation with censoring. It should be noted that we set a truncation value that corresponds to the upper nearest integer $\lceil 2\sqrt{n} \rceil$ observation, i.e., $x_0 = x_{\lceil 2\sqrt{n} \rceil}$ where n is the total number of observations. A similar approach is used in [87,88].

It is noted that, for the estimation of ELEs, it is assumed that traffic follows a stationary process. This assumption is based on previous studies, for example, [19,89,90], which show that the increase in traffic volume and the proportion of heavy trucks have an insignificant impact on the predicted ELEs. Specifically, at a 20-year return period, the increase in predicted ELEs is insignificant. Whereas, at a 75-year return period, the increase is generally moderate. Additionally, when using the GEV distribution to model the maximum LE values, the shape and scale parameters do not vary significantly over time despite traffic growth. Sampling-based extreme value analysis is the most straightforward approach for accurate time-variant reliability assessment [91].

To sum up, extreme value analysis is performed to estimate the ELEs. Six parametric distribution fits are applied to the daily maxima load effects per bridge. These distributions are Gumbel (Gumbel), two-parameters Weibull (Weibull₂), three-parameters Weibull (Weibull₃); and the corresponding fitted distributions with truncated likelihood function of x_0 , Gumbel _{x_0} , Weibull_{2; x_0} and Weibull_{3; x_0} .

2.5. Bridge criticality

The criticality of the bridge, as defined in this paper in Eq. (4), refers to the ratio (r) between the extreme traffic load effect observed (LE_D) and the characteristic load effect induced by the design live load model (LE_D). Consequently, r can serve as a meaningful load effect bridge performance indicator. For example, in the case study mentioned earlier in Section 2.1.1, it was found that the design of 414 bridges took into account the AASHTO standards for live loads [45], specifically the HS15–44 and HS20–44 vehicles. These vehicles consist of a semitrailer truck with a gross vehicle weight of 240.2 kN and 320.2 kN,

respectively, or an equivalent lane load (see Fig. A.3(a)). To compute the characteristic values, the type of loading to be used (truckload or lane load) will be the one that generates the maximum load effect. The remaining 162 bridge structures were designed using the Mexican six-axle HVs T3-S3 and nine-axle HV T3-S2-R4 with their corresponding maximum allowable loads established in [52]. It is worth mentioning that these live loads are based neither on probabilistic analysis of traffic loads nor on bridge structural capacity but on road capacity. In order to identify the most critical bridges in the network, an analytical comparison is conducted between the actual ELEs and the characteristic values resulting from the design live loads. Locations where a value of r exceeds one indicate that the estimated ELE surpasses the characteristic value specified by the corresponding live load model. In such cases, the bridges are considered critical due to the potential for load exceedance.

$$r = \frac{LE_O}{LE_D} \quad (4)$$

3. Illustrative example application to a specific bridge

The proposed framework is applied to the entire MHC network. For the sake of illustration, specific results for a selected bridge are presented in this section. Results at a network level are discussed in Section 4. The bridge *El Rosario I* is studied in the following illustrative example application. The characteristics of the traffic data for the site are first described. Site-specific traffic simulation is next performed. Later the load effects are computed and finally, the load effects are analysed and ELEs are estimated.

According to the SIPUMEX database, *El Rosario I* is a two-lane nine-span continuous bridge with a total length of 264.4 m. It has a minimum span length of 25.8 m and a maximum span length of 30.8 m. Built in 1982, the bridge is located in the state of Baja California Sur on the MHC number 6 *Transpeninsular Baja California*. The nearest counting station is *Rosario de Arriba* located around 4 km west over the same MHC. The annual average daily truck traffic that circulates by this station is 444 HVs with the following configuration: 45% C2, 9.7% C3, 43% T3S2, 1.4% T3S3 and 0.9% T3S3R4. This information serves as input for the GCBN model. According to the notation introduced in Section 2.2.1, in *El Rosario I* bridge ($b = 9$), with information of the counting station *Rosario de Arriba* ($c = 60$), the five vehicle types presented in Table 2 are registered, i.e., $K_{60}^9 = 5$. Hence the vehicle types that conform to the traffic flow are $I_{60}^9 = \{C2, C3, T3S2, T3S3, T3S2R4\}$. Their corresponding proportions $p_{60,i}^9$ of the total vehicles are: $p_{60,1}^9 = 0.45$, $p_{60,2}^9 = 0.097$, $p_{60,3}^9 = 0.43$, $p_{60,4}^9 = 0.014$ and $p_{60,5}^9 = 0.009$. The corresponding site-specific direct acyclic graph that represents the GCBN₆₀⁹ model is shown in Fig. 3.

We compute $N_{60}^9 = AADTT_{60}^9 = 444$ un-conditional samples using the GCBN₆₀⁹ model. The inter-vehicle gaps are simulated using the approach described in Section 2.2.2. The output is a database of the synthetic site-specific traffic load observations (different every time the model is run). Table A.3 presents the generated synthetic traffic of one day and Fig. A.1 shows the corresponding bar plot of the number of HVs simulated per hour for lane 1 of the bridge *El Rosario I*.

Once the synthetic traffic is computed, the load effects of interest for each vehicle are calculated according to the procedure described in Section 2.3 and the envelope of the results is found. The absolute maximum values of the bending moments and shear forces envelopes per day obtained are stored. In total 200 days are simulated. Therefore 200 daily maxima load effects are obtained. The resulting envelopes of one day of the bending moments are presented in Fig. 6.

As described in Section 2.4, the ELEs are computed with a return period of 50 years and 1000 years according to the specifications [92, 93] correspondingly. As stated in [94], it is considered that there are 254 working days excluding weekends and holidays in Mexico. The daily absolute maxima load effects are fitted to the selected parametric distributions. Fig. 7 shows the comparison of the fitted distributions presented in Section 2.4 for the absolute bending moment for bridge *El Rosario I*. The parametric distributions Weibull₂ and Gumbel produce significantly lower characteristic values for this particular case. A vi-

sual inspection suggests that the best fit is provided either by Gumbel_{x₀} or Weibull_{3;x₀} with $x_0 = 2838.4$ kN m. However, using the Akaike Information Criterion (AIC) [95] to measure the quality of the fitting, Weibull₃ (black dashed line in Fig. 7) is the selected distribution that better describes the data. The estimated extreme bending moments are 3614 kN m and 3766 kN m with 50-year (M_{50}) and 1000-year (M_{1000}) return periods, respectively. When analysing the absolute shear force for the same bridge, the best fit is provided by Weibull_{2;x₀} with $x_0 = 681.7$ kN. The estimated extreme shear forces are 928 kN and 1011 kN with 50-year (V_{50}) and 1000-year (V_{1000}) return periods accordingly.

Finally, the load effect bridge performance indicator (Section 2.5), denoted as r is computed to evaluate the performance of the bridge under consideration. According to the SIPUMEX database, for the design of the bridge, the AASHTO standard truck HS20-44 model is used as the representative design live load model. The maximum bending moment induced by the design live load model (M_D) amounts to 4501.4 kN m. Additionally, the maximum shear force caused by the same design live load model (V_D) corresponds to 928.1 kN. Subsequently, the load effect performance indicator for the bending moment, considering a 50-year return period is $M_{50,r} = M_{50}/M_D = 3614/4501 = 0.80$. Similarly, the load effect performance indicator for the shear force is $V_{50,r} = V_{50}/V_D = 928/982 = 0.95$. When the obtained performance indicators are contrasted with the load effects corresponding to a 1000-year return period, the resulting ratios for the bending moment and shear force are 0.84 and 1.03, respectively. These ratios are denoted as $V_{1000,r}$ and $M_{1000,r}$.

4. Extreme load effects at a network level

The methodology explained in Section 2 and illustrated in Section 3 is applied to the 576 bridges of the MHC. Over 159 million HVs are simulated using 278 site-specific GCBNs. The loading effect on the respective bridge of each HVs has been calculated. This long-run traffic load simulation involves a high computational cost of around 13 000 core hours, performed on the DelftBlue supercomputer at TU Delft [96]. Out of the 576 maximum 254-day load effects computed, 529 are caused by individual HVs and 47 by a convoy of vehicles. For illustration purposes, Fig. A.2 shows the vehicle types that caused the maximum 254-day absolute bending moment and the corresponding GVW distribution of the first two lanes of all bridges. Notice that around 96% of the studied bridges have two lanes. A bi-modal-like distribution can be observed for the GVW with two peaks at around 580 kN and 950 kN. These values are likely to be due to the vehicles meeting the maximum allowable GVW and overweight vehicles, correspondingly. The max GVW according to Mexican standards [52] is 740.41 kN. The vehicle types C2 and C3 caused the maximum bending moment in only five bridges.

Extreme value analysis is performed on each one of the bridges under study to find the characteristic values of the load effects. In order to select a particular distribution for the maximum at each bridge AIC together with visual inspection was used. AIC values for different parametric distributions vary significantly between bridge structures mainly due to the large variation in moments and shear forces calculations across bridges (notice that for all bridges 254 daily maxima are used). In general, mostly the Weibull₃ distribution and the Weibull_{2;x₀} distribution are the ones that better describe the individual daily maxima load effects.

Once all the distributions that better describe the data are selected, the ELEs M_{50} , M_{1000} , V_{50} and V_{1000} are estimated for the 576 bridges. Let E denote a random variable representing any of the four estimated ELEs. The resulting ELEs are categorized into 6 classes according to: $[E_{\min}, E_5]$, $[E_5, E_{25}]$, $[E_{25}, E_{50}]$, $[E_{50}, E_{75}]$, $[E_{75}, E_{95}]$ and $[E_{95}, E_{\max}]$. Where E_q denotes the q th percentile of the distribution of E . As an example, the ELE M_{50} map is presented in Fig. 8, to increase legibility, simple geometric square markers are used to represent individual bridges. The colour code of the geometric markers represents each of the 6 M_{50} percentile classes. For this example the 6 classes are (in kN m): [592, 800), [800, 1327), [1327, 2507), [2507, 4918), [4918, 9320)

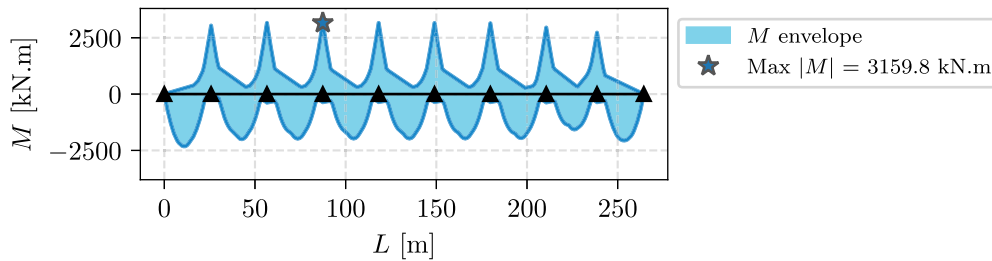


Fig. 6. Load effects envelopes for the continuous bridge *El Rosario I* corresponding to one day of traffic simulation. Envelope of bending moments.

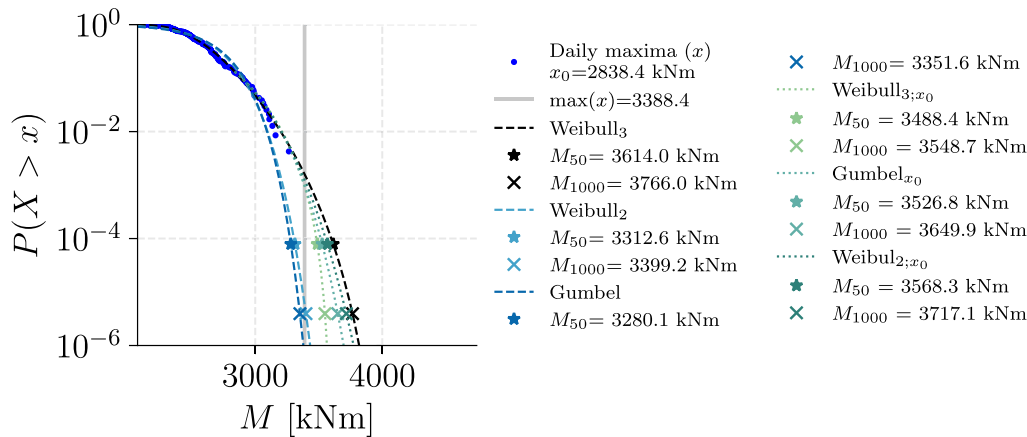


Fig. 7. Exceedance probability plot comparison bridge *El Rosario I*. In blue circles, the absolute bending moment daily maxima values. The vertical grey solid line represents the value of the maximum daily maxima recorded observation. The star markers represent the extrapolated value that corresponds to an ELE with a 50-year (M_{50}). The triangle markers represent an ELE with a 1000-year (M_{1000}) return period. (For interpretation of the references to colour in this figure legend, the reader is referred to the web version of this article.)

and [9320, 16 124]. The corresponding histogram of frequencies of the computed M_{50} distribution is presented at the bottom of the figure. The highest extreme bending moment with a return period of 50 years (1623.8 kN m) corresponds to the 7-span bridge *Rio Fuerte* located in the northwest region of Sinaloa state (star shape maker in Fig. 8). This result is expected since *Rio Fuerte* bridge has one of the largest spans of the database (44.7 m). A similar map for V_{50} can be found in Fig. A.6 in the Appendix. Mapping the site-specific extreme traffic load effects allows the identification of the most critical bridges for which more detailed information or immediate traffic-related actions may be required.

4.1. Comparison with a simple popular method

When applying Turkstra’s Rule it is assumed that the trucks meet at the critical point of the influence line, which represents an extreme loading event. However, the extreme loading events consist of very heavy trucks meeting near, but not exactly at, this critical point. Therefore, as pointed out by [97] a more intuitive model would consider placing one of the trucks at a distance αL from the other, where α represents a scaling factor (see Fig. A.3). It is important to note that the situation differs for the two load effects, resulting in α_M not being equal to α_V .

Through the analysis of simulations that generate the maximum daily load effects for simply supported two-lane bridges (total of 445 bridges), the application of Turkstra’s Rule reveals that the 50-year loading event consists of the 50-year truck in the slow lane, combined with the one-day return period truck for 280 bridges and the one-week return period truck for the remaining bridges. The values of $\alpha_{M_{50}}$ range from 0.02 to 0.70, while $\alpha_{V_{50}}$ varies between 0.06 and 0.89. The selection of α_M and α_V values was based on achieving the closest approximation to the target values, specifically M_{50} and V_{50} obtained from the simulations. Based on this investigation, it can be concluded that in 362 out of the 445 two-lane bridges, the (extended) Turkstra’s Rule yields accurate results with discrepancies ranging from -0.3% to

$+3.0\%$ for M_{50} . Conversely, for V_{50} , the variations range from -0.3% to $+3.9\%$ for the same set of bridges. On the other hand, discrepancies of up to 15.8% and 23.0% are obtained when comparing the values of M_{50} and V_{50} , respectively, in cases where Turkstra’s Rule fails to produce precise outcomes for bridge analysis.

As can be seen, Turkstra’s Rule simplified model provides accurate estimations of the ELEs in the majority of the studied bridges. Nevertheless, a trial-and-error approach is needed to derive the value of alpha. Moreover, the computation of site-specific 50-year trucks requires extensive simulations. While it is conceivable to construct a moderately precise model through this method, it is essential to note that the process is both highly dependent on site-specific factors and time-intensive. Extending Turkstra’s Rule model to include continuous bridges and three or more lanes is beyond the scope of this paper. However, future works will explore the differences between Turkstra’s Rule model and our approach, specifically incorporating continuous bridges and three or more lanes.

4.2. Mapping bridge criticality

In this section, as mentioned in Section 2.5 to identify the most critical bridges on the network, a load effect bridge performance indicator based on the ratio r between the computed extreme load effects and the design load effects is computed. The obtained ELEs are compared with the characteristic values calculated using the reported design live load (HS15-44, HS20-44, T3-S3 or T3-S2-R4) at each bridge site. According to [45], it is assumed that the standard trucks occupy a width of 3.00 m. In load factor design, a live load factor of 1.67 is adopted. Additionally, a reduction of the live load of 90% and 75% may be used in view of improbable coincident loadings for three lanes and for four lanes or more, respectively. Because of the absence of a Mexican bridge design code, the live load factor and live load reductions due to the improbable coincident loadings in lanes established in the AASTHO standards are assumed.

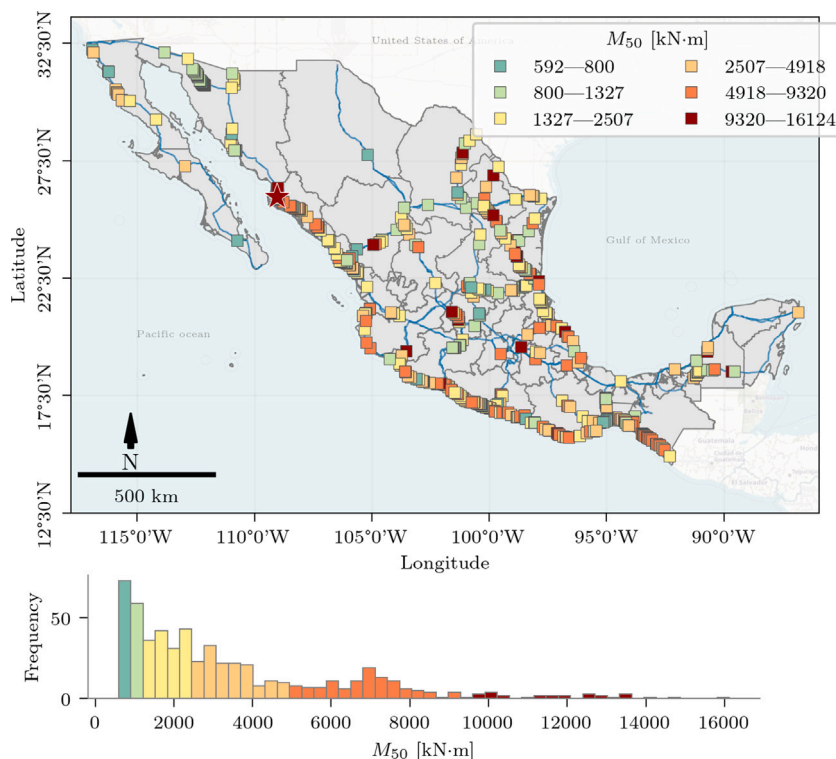


Fig. 8. Extreme load effects map for the maximum absolute bending moment with a 50-year return period. (For interpretation of the references to colour in this figure legend, the reader is referred to the web version of this article.)

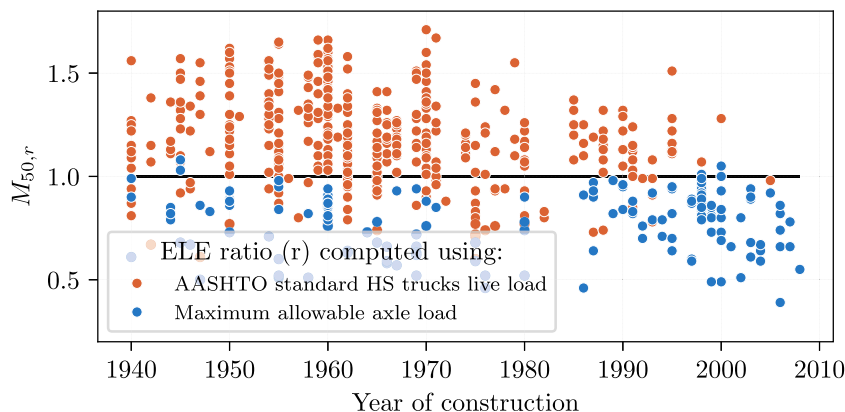


Fig. 9. Computed extreme load effects ratios per bridge per year. Maximum absolute bending moment with 50-year return period ratios ($M_{50,r}$).

Fig. 9, shows the computed 50-year absolute bending moment ratios, $M_{50,r}$, for all bridges under study. These ratios indicate that, in most cases, the $M_{50,r}$ values are significantly higher when compared to those generated by the AASHTO standard HS truck live loads. Specifically, they can be up to 1.71 times larger for bending moments (similarly, up to 1.67 times larger for shear forces). On the other hand, when considering the ratios computed with the maximum allowable Mexican HVs, a different trend emerges. In this case, the load effects computed using the maximum allowable values specified in the Mexican standard exceed those computed using our approach, which is based on observed data. Therefore, Fig. 9 reveals that the computation of ELEs ratios on bridges subjected to AASHTO loads results, usually, in lower load effects than when considering Mexican allowable HVs. Notice that the ratio decreases as the year of construction progresses. The results of the ratios presented above are in line with the fact that the AASHTO standard HS trucks, which were commonly used until the early 2000s for the structural design of bridges in Mexico,

underestimate the values of the load effects (shear forces and bending moments) for design [98,99]. As a result, in 2001 the Mexican Institute of Transportation proposed a live load model named IMT-66.5 [92] better aligned with the actual traffic load demands.

The computed ratios are categorized into 6 classes according to the 5th, 25th, 50th, 75th, and 95th percentiles of the corresponding distribution, i.e., $[r_{min}, r_5)$, $[r_5, r_{25})$, $[r_{25}, r_{50})$, $[r_{50}, r_{75})$, $[r_{75}, r_{95})$ and $[r_{95}, r_{max}]$. For illustration, Fig. 10 presents the ratios $M_{50,r}$ map. A similar map of $V_{50,r}$ can be found in Fig. A.9. As can be seen, the lowest ratio values for both extreme traffic load effects (between 0.41 and 0.67) are mostly concentrated on the bridges located on corridors that cross the states of Sinaloa, Guanajuato, and Guerrero accordingly. The ratio is approximately 1–1.3 in most parts of the major corridors highway network. The highest ratios (above 1.42) are primarily concentrated on the highway that connects the cities of Caborca and Sonoyta in northern Mexico. In order to exemplify a simple use of maps as a tool, a characterization of the computed load effect indicators is presented in the following section.

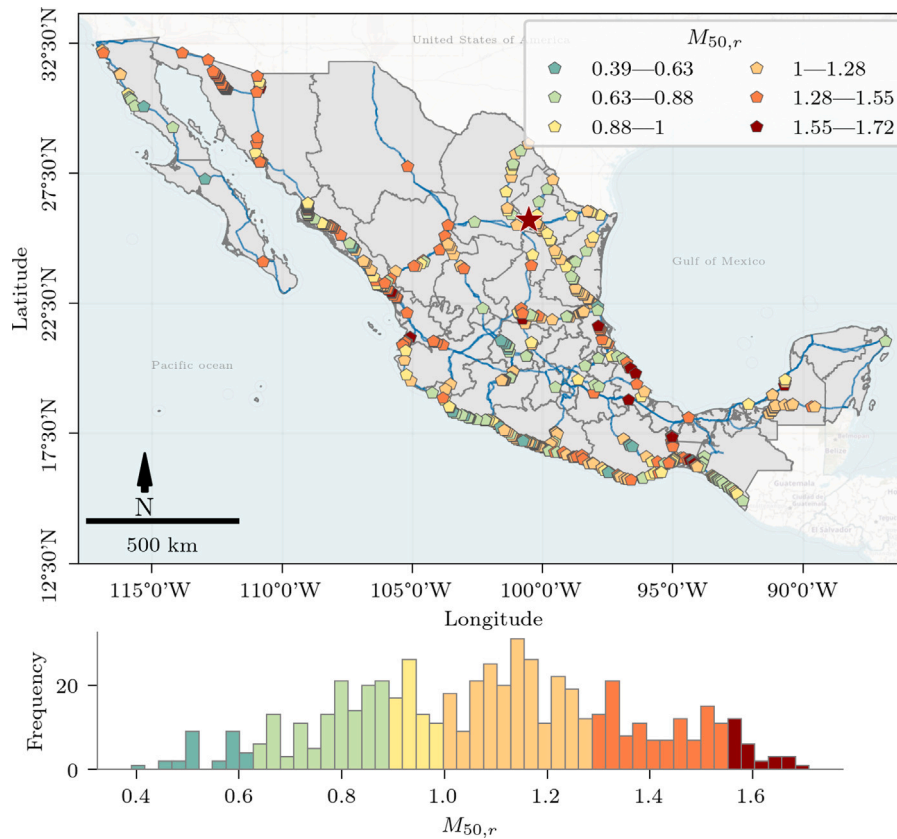


Fig. 10. Extreme bending moment with 50-year return period ratios ($M_{50,r}$). Each pentagon shape marker represents a computed ratio per bridge. The star marker represents the bridge with the highest $M_{50,r}$ corresponding to Arboledas bridge $M_{50,r} = 1.71$.

4.3. Comparison of bridge criticality at major highway corridors

In order to perform a load effect bridge criticality characterization, the fifteen MHCs, shown in Fig. A.4, were considered. The percentage of bridges with r considering load effects with a 50-year return period greater than one, i.e. $\%M_{50,r} > 1$ and $\%V_{50,r} > 1$ are presented in Fig. 11 for all corridors. It can be observed that both indicators have similar behaviour with the exception of corridor number 14 in which the $\%M_{50,r} > 1$ is more than double the $\%V_{50,r} > 1$ (89%–39%). The highest $\%M_{50,r} > 1$ values are presented in the MHC *Península de Yucatán* (corridor number 14, 89%), *Circuito Transistmico* (corridor number 13, 76%) and *México-Nogales, Tijuana* (corridor number 1, 71%) Whereas the highest $\%V_{50,r} > 1$ can be found in corridors number 1, 7 (*Acapulco-Veracruz*) and 13. In addition, corridors *México-Tuxpan* and *Altiplano* presented a value of 0% due to the fact that these corridors have few bridges, 2 and 3 bridges respectively. Among the MHCs, it is clear that MHC number 14 is the corridor where attention is needed since the estimated characteristic loading in 16 out of its 18 bridges is greater than the design values specified by the corresponding live load model reported in SIPUMEX database. With 145 bridges in total, *México-Nogales, Tijuana* (MHC number 1) is the corridor with more bridges in the Mexican Federal highway network. This corridor is another point of attention since 103 of its bridges have a $\%M_{50,r} > 1$ and 93 bridges (64%) a $\%V_{50,r} > 1$. It is likely that perturbations on the bridges of these corridors will generate certain stress levels in their road network generating at least an increase in user travel costs. Notice that by omitting corridors number 4 and number 10 the average percentage of bridges with $\%M_{50,r} > 1$ is 62% and the average $\%V_{50,r} > 1$ is 46.5%. It is clear that more than half of the existing bridges in the network need attention.

The previous description was focused on 50-year LEs, but the trends are also representative of other return periods. In contrast to the Mexican standards, in the Eurocode EN 1991-Part 2: Traffic load on bridges [93] the characteristic values are defined with a return period of 1000 years instead of 50 years due to the requirement of

serviceability and sustainability of the structures. For example, when considering bending moments with a 1000-year return period, the number of bridges in the most critical group (ratios between 1.55 and 1.72) increases from 31 to 68. As can be seen, the return period is a crucial factor in risk analysis and design. Events with low probabilities may result in greater casualties, direct losses, and indirect effects. The corresponding maps of ELEs with a return period of 1000 years can be found in the Appendix (Figs. A.5, A.7, A.8 and A.10). Additionally, the supplementary material presents individual maps for M_{50} , V_{50} , $M_{50,r}$, and $V_{50,r}$ for each MHC. An interactive map has also been produced using QGIS. The map can be accessed at https://mike-mendoza.github.io/eles_mexico/.

As illustrated, the methodology and maps presented help to visually identify changes, trends, and hot spots that may require attention on a large bridge network. For the Mexican authorities, the maps delivered herein give the first clear picture of the distribution of extreme load effects on concrete bridges due to traffic loads at the Mexican highway network. They provide relevant information that can support the development of a comprehensive approach to bridge management to prioritize structural inspection or maintenance interventions.

5. Conclusions

This paper has presented a 4-step method to estimate and map the extreme bending moments, extreme shear forces, and load effect performance indicators due to traffic in a bridge network at a national scale as realistically and accurately as possible when information is scarce. This approach permits the visualization and measurement of the criticality of elements in the network. Hence, to some extent, the degree to which individual bridges require attention. The criticality of the bridge, as described in this research, relates to the relationship between the chosen extreme traffic load effect and the load effect caused by the design live load model.

The method is low information-intensive per bridge. The necessary information in most cases is usually available in countries with a

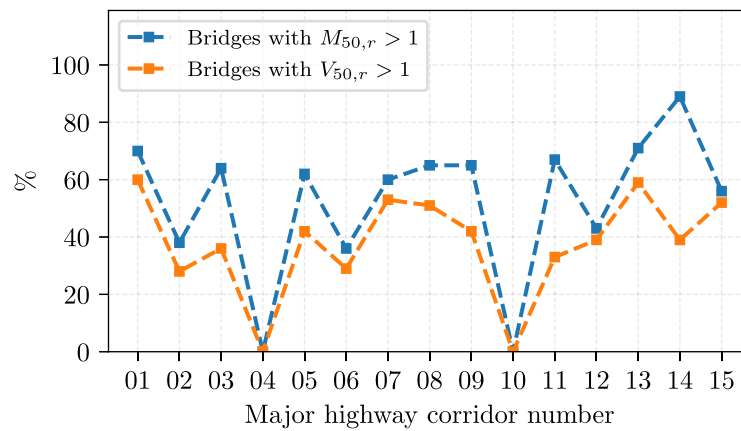


Fig. 11. Percentage of bridges with a $M_{50,r}$ and $V_{50,r}$ above 1 per major highway corridor.

least one-module bridge management system. Regarding the bridge data, it requires the number of spans and the corresponding length, the number of lanes and the corresponding width, and the design live load. Regarding traffic information, the method requires the Annual Average Daily Traffic and the proportion per vehicle type that conforms the traffic flow.

The method uses Gaussian copula-based Bayesian Networks to generate site-specific synthetic observations of heavy vehicles. To simulate traffic flow a copula-based approach is used to characterize the inter-vehicle gap by estimating its auto-correlation. A long-run traffic load simulation is used to obtain the traffic load effects on the bridges. Then, the extreme load effects are estimated using the block maxima extreme value analysis approach. The comparison of the obtained values with the design loads reveals interesting information about the criticality of the existing infrastructure. To illustrate the method, it has been applied to a case study involving the bridge network located along the fifteen major toll-free highway corridors in Mexico, which comprises a total of 576 bridges. The results of this study were then used to create four main maps that provide a comprehensive understanding of the load effects on the bridges within a national highway network, enabling the identification of spatial patterns and relationships. It is recommended to draw attention to bridges with values of bridge criticality greater than one. These assets require comprehensive and more reliable inspections.

The main advantages of this methodology include its simplicity and ease of application due to its straightforward conceptualization. Additionally, the required data can be obtained from basic information about the bridges and traffic, as well as publicly available databases, making it highly flexible and applicable to nearly any bridge network. This study encounters certain limitations. Firstly, it relies on a restricted amount and variety of data from a specific bridge network. Therefore, it does not take into account factors such as the impact of ageing on individual bridge structures and bridge component ratings. Secondly, the computational cost of the method increases proportionally with the number of bridges under consideration, making complex structural analyses resource-intensive and demanding extensive material and geometrical data. Lastly, the approach used to estimate characteristic values of load effects primarily relies on the block maxima extreme value analysis method. The sensitivity of the results to a different choice (Peaks-Over-Threshold method for example) has not been tested. However, the goal was to develop a universal, simple method to aid local authorities in regions where WIM systems are not the primary source of traffic data. It is important to note that this paper acknowledges the limitations of existing traffic data sources and emphasizes the crucial role of collecting additional data through WIM systems. Therefore, it does not suggest that WIM traffic data is unnecessary but rather advocates for its use to obtain reliable results in traffic loading analysis by collecting accurate and substantial amounts of traffic data.

Future work based on the methodology can investigate its applicability in other networks to test its ability as a general approach. Regions in the United States and Europe in which data from robust BMS and WIM systems are available can be used to apply the methodology in its corresponding networks. It is possible, for instance, to quantify a BN model with WIM datasets and analyse its performance relative to the Mexican quantification presented in this paper, as well as to combine those data. In this manner, several scenarios can be made with an increase in traffic volume and different vehicle configurations passing through specific bridges. Further research can explore the use of different approaches for estimating ELEs. In particular, the Peaks-Over-Threshold method seems like a natural starting point. Additionally, consider the integration of WIM data from diverse regions to assess its influence on the bridge criticality results. Finally, researchers could explore ways to integrate the methodology into decision-making processes by combining bridge performance measurements such as condition rating and bridge criticality presented here to optimize preventive maintenance schedules of all the bridges of the network.

CRediT authorship contribution statement

Miguel Angel Mendoza-Lugo: Conceptualization, Data curation, Formal analysis, Funding acquisition, Investigation, Methodology, Software, Validation, Visualization, Writing – original draft, Writing – review & editing. **Maria Nogal:** Conceptualization, Formal analysis, Investigation, Methodology, Resources, Supervision, Validation, Writing – review & editing. **Oswaldo Morales-Nápoles:** Conceptualization, Formal analysis, Investigation, Methodology, Project administration, Resources, Supervision, Writing – review & editing.

Declaration of competing interest

The authors declare that they have no known competing financial interests or personal relationships that could have appeared to influence the work reported in this paper.

Data availability

Data will be made available on request.

Acknowledgements

This research was supported by the Mexican National Council for Science and Technology (CONACYT) under project number 2019-000021-01EXTF-00564 CVU 784544.

Appendix A

See Tables A.1, A.2, A.3(a) and A.3(b) and Figs. A.1.

Table A.1

Inter-axle distances (D) general statistics, mean and coefficient of variation (cv) comparison. Reported (Rep.) in [63] and simulated (Sim.).

Type	Statistic	D_{1-2}		D_{2-3}		D_{3-4}		D_{4-5}		D_{5-6}		D_{6-7}		D_{7-8}		D_{8-9}	
		Rep.	Sim.	Rep.	Sim.	Rep.	Sim.	Rep.	Sim.	Rep.	Sim.	Rep.	Sim.	Rep.	Sim.	Rep.	Sim.
C2	Mean	528.12	529.54	-	-	-	-	-	-	-	-	-	-	-	-	-	-
	cv	0.71	0.19	-	-	-	-	-	-	-	-	-	-	-	-	-	-
C3	Mean	502.42	502.56	127.22	128.98	-	-	-	-	-	-	-	-	-	-	-	-
	cv	0.10	0.11	0.06	0.07	-	-	-	-	-	-	-	-	-	-	-	-
T3S2	Mean	452.39	452.80	135.99	134.72	818.04	837.25	115.11	129.19	-	-	-	-	-	-	-	-
	cv	0.12	0.14	0.07	0.10	0.17	0.11	0.09	0.07	-	-	-	-	-	-	-	-
T3S3	Mean	545.81	455.43	136.74	135.31	657.99	661.64	119.01	128.73	117.43	128.84	-	-	-	-	-	-
	cv	0.09	0.14	0.70	0.04	0.16	0.11	0.08	0.07	0.08	0.08	-	-	-	-	-	-
T3S2R4	Mean	481.79	455.12	141.95	137.82	672.76	653.05	122.27	128.87	238.21	197.12	118.88	129.07	591.94	577.82	110.78	129.05
	cv	0.10	0.21	0.07	0.12	0.28	0.08	0.16	0.08	0.08	0.07	0.20	0.07	0.20	0.15	0.10	0.07

Table A.2

Fitted copulas of the auto-correlated time series for weekday number 16^a.

Hour	Copula	Name	θ	ρ	Number of observations
0	$C_{\theta_y}^{16,0}\{F(y_t), F(y_{t-1})\}$	Clayton	0.08	0.06	91
1	$C_{\theta_y}^{16,1}\{F(y_t), F(y_{t-1})\}$	Frank	-1.01	-0.17	82
2	$C_{\theta_y}^{16,2}\{F(y_t), F(y_{t-1})\}$	Joe	1.07	0.06	129
3	$C_{\theta_y}^{16,3}\{F(y_t), F(y_{t-1})\}$	Joe 270° rotated	1.05	-0.05	275
4	$C_{\theta_y}^{16,4}\{F(y_t), F(y_{t-1})\}$	Frank	-0.41	-0.08	622
5	$C_{\theta_y}^{16,5}\{F(y_t), F(y_{t-1})\}$	Frank	-0.66	-0.11	559
6	$C_{\theta_y}^{16,6}\{F(y_t), F(y_{t-1})\}$	Frank	-0.72	-0.13	387
7	$C_{\theta_y}^{16,7}\{F(y_t), F(y_{t-1})\}$	Frank	0.18	0.03	439
8	$C_{\theta_y}^{16,8}\{F(y_t), F(y_{t-1})\}$	Frank	-0.29	-0.05	482
9	$C_{\theta_y}^{16,9}\{F(y_t), F(y_{t-1})\}$	Clayton 270° rotated	0.03	-0.02	505
10	$C_{\theta_y}^{16,10}\{F(y_t), F(y_{t-1})\}$	Frank	-0.17	-0.03	443
11	$C_{\theta_y}^{16,11}\{F(y_t), F(y_{t-1})\}$	Clayton 180° rotated	0.07	0.05	449
12	$C_{\theta_y}^{16,12}\{F(y_t), F(y_{t-1})\}$	Frank	-0.41	-0.08	492
13	$C_{\theta_y}^{16,13}\{F(y_t), F(y_{t-1})\}$	Gumbel 90° rotated	1.06	-0.09	400
14	$C_{\theta_y}^{16,14}\{F(y_t), F(y_{t-1})\}$	Frank	-0.24	-0.05	387
15	$C_{\theta_y}^{16,15}\{F(y_t), F(y_{t-1})\}$	Gaussian	-0.11	-0.11	334
16	$C_{\theta_y}^{16,16}\{F(y_t), F(y_{t-1})\}$	Frank	0.33	0.06	308
17	$C_{\theta_y}^{16,17}\{F(y_t), F(y_{t-1})\}$	Clayton 270° rotated	0.22	-0.16	190
18	$C_{\theta_y}^{16,18}\{F(y_t), F(y_{t-1})\}$	Clayton 180° rotated	0.12	0.09	151
19	$C_{\theta_y}^{16,19}\{F(y_t), F(y_{t-1})\}$	Clayton 270° rotated	0.03	-0.03	100
20	$C_{\theta_y}^{16,20}\{F(y_t), F(y_{t-1})\}$	Clayton	0.04	0.03	93
21	$C_{\theta_y}^{16,21}\{F(y_t), F(y_{t-1})\}$	Joe	1.10	0.09	83
22	$C_{\theta_y}^{16,22}\{F(y_t), F(y_{t-1})\}$	Clayton 90° rotated	0.36	-0.23	79
23	$C_{\theta_y}^{16,23}\{F(y_t), F(y_{t-1})\}$	Clayton 90° rotated	0.28	-0.19	79

^a Notice that low correlations are observed in the majority of the hours throughout the day. This observation suggests relatively independent behaviour during different hours of the day. This could indicate that the occurrence of events or patterns on this particular weekday is not strongly influenced by the time of day. However, since the empirical data observations are limited in quantity, the fitted copula models are used to generate additional synthetic observations.

Table A.3(a)

Example of a random realization (output) of the synthetic traffic for the bridge *El Rosario I*. The first column in the table represents the ID of the synthetic observation, the second the vehicle type, the third the gross vehicle weight in kN and columns 4 to 12 the individual axle load (A) in kN.

ID	Type	GVW	A1	A2	A3	A4	A5	A6	A7	A8	A9
0	T3S2	157.20	30.01	34.33	34.57	30.69	27.61	-	-	-	-
1	T3S2	315.58	34.81	73.55	69.13	71.22	66.87	-	-	-	-
⋮	⋮	⋮	⋮	⋮	⋮	⋮	⋮	⋮	⋮	⋮	⋮
208	C3	137.40	34.87	39.18	63.35	-	-	-	-	-	-
209	T3S2	231.84	47.70	47.29	34.74	52.82	49.30	-	-	-	-

Table A.3(b)

The first column of this table corresponds to the 13th column of [Table A.3\(a\)](#) representing the total length of the HV in meters, columns 14 to 22 represent individual inter-axle distances (D in m), and the last column the inter-vehicle gap (IVG in m.)

Length	D1	D2	D3	D4	D5	D6	D7	D8	D9	IVG
16.76	1.78	3.81	5.62	1.31	1.31	-	-	-	-	-
15.95	1.91	3.71	4.77	1.79	1.79	-	-	-	-	606.07
⋮	⋮	⋮	⋮	⋮	⋮	⋮	⋮	⋮	⋮	⋮
8.37	0.84	4.33	1.02	-	-	-	-	-	-	542.97
16.55	1.76	3.73	5.56	1.32	1.32	-	-	-	-	464.49

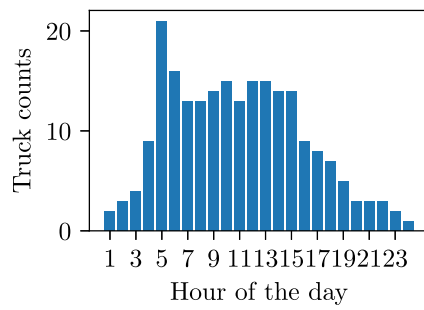


Fig. A.1. One random simulation of 24 h of traffic flow of bridge *El Rosario I* Lane 1.

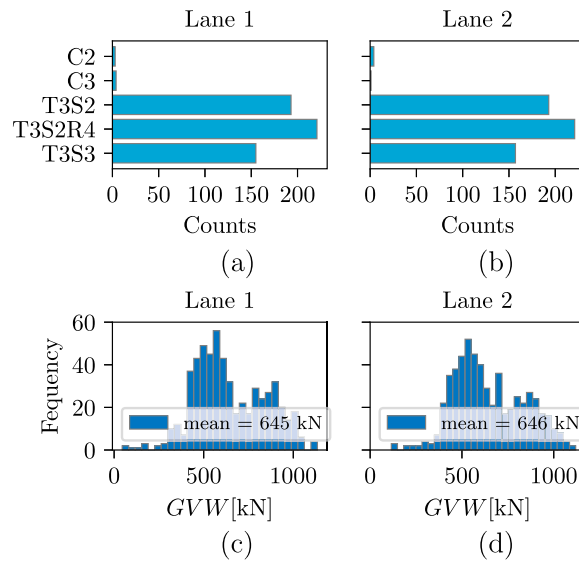


Fig. A.2. Lanes 1 and 2 distributions of vehicle types that caused the maximum 200-day absolute bending moment for the studied bridges. (a)–(b) Bar plot of individual vehicle type counts. (c)–(d) Gross vehicle weight histogram.

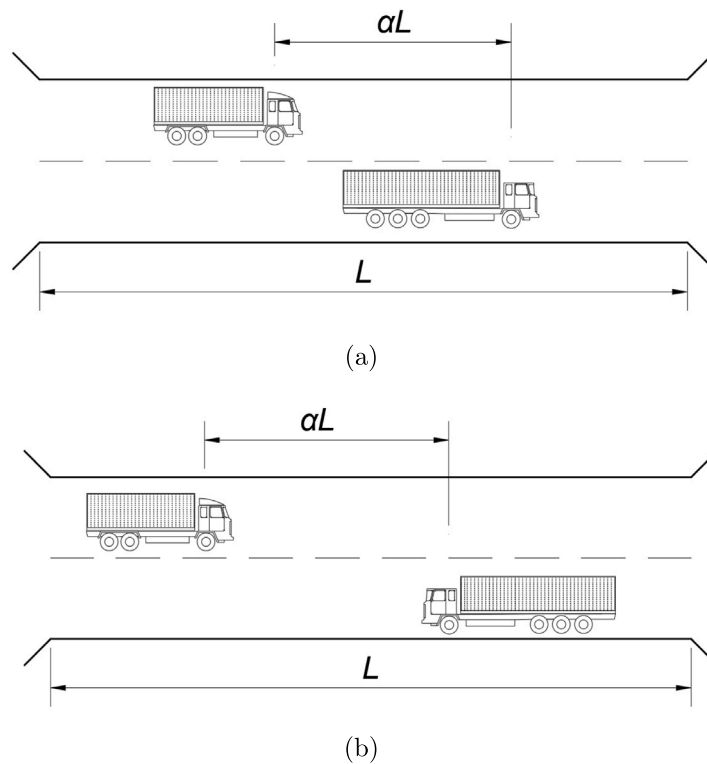


Fig. A.3. Traffic scenario that causes the extreme loading event for two-lane simple supported bridges. (a) same direction lanes, (b) opposite direction lanes.

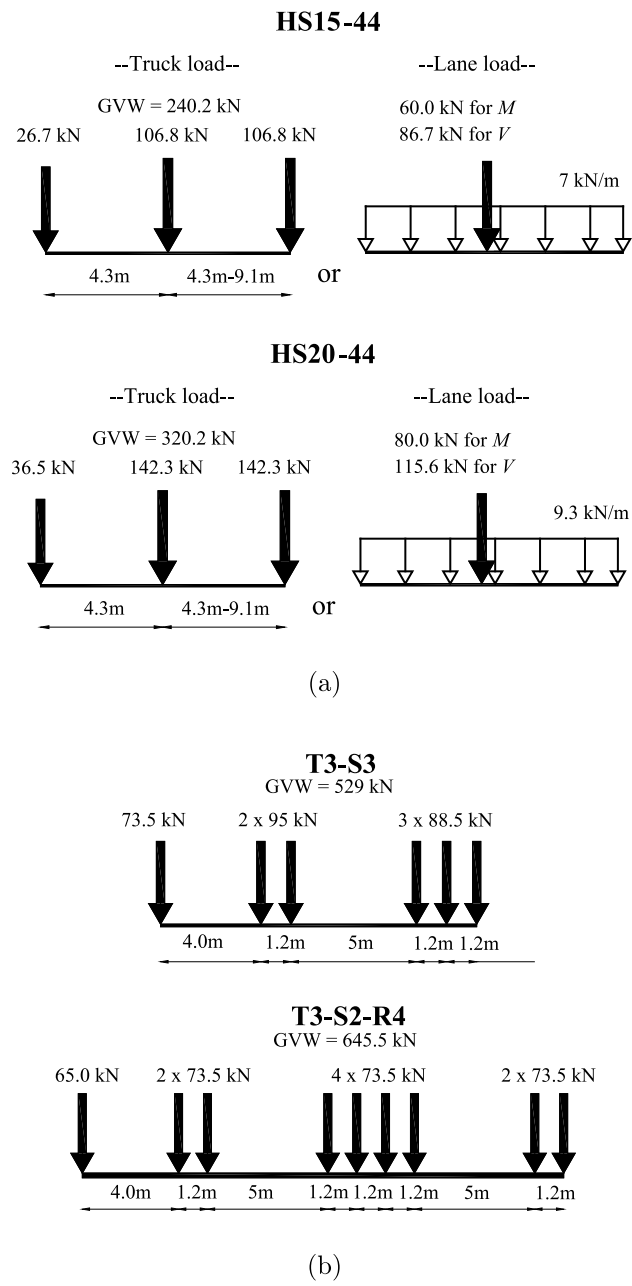


Fig. A.3. Traffic live load models reported in SIPUMEX database (a) AASHTO standard HS Trucks and lane loadings, (b) Maximum allowable axle loads for the trucks types T3-S3 and T3-S2-R4.



Fig. A.4. Major highway corridors of Mexico.

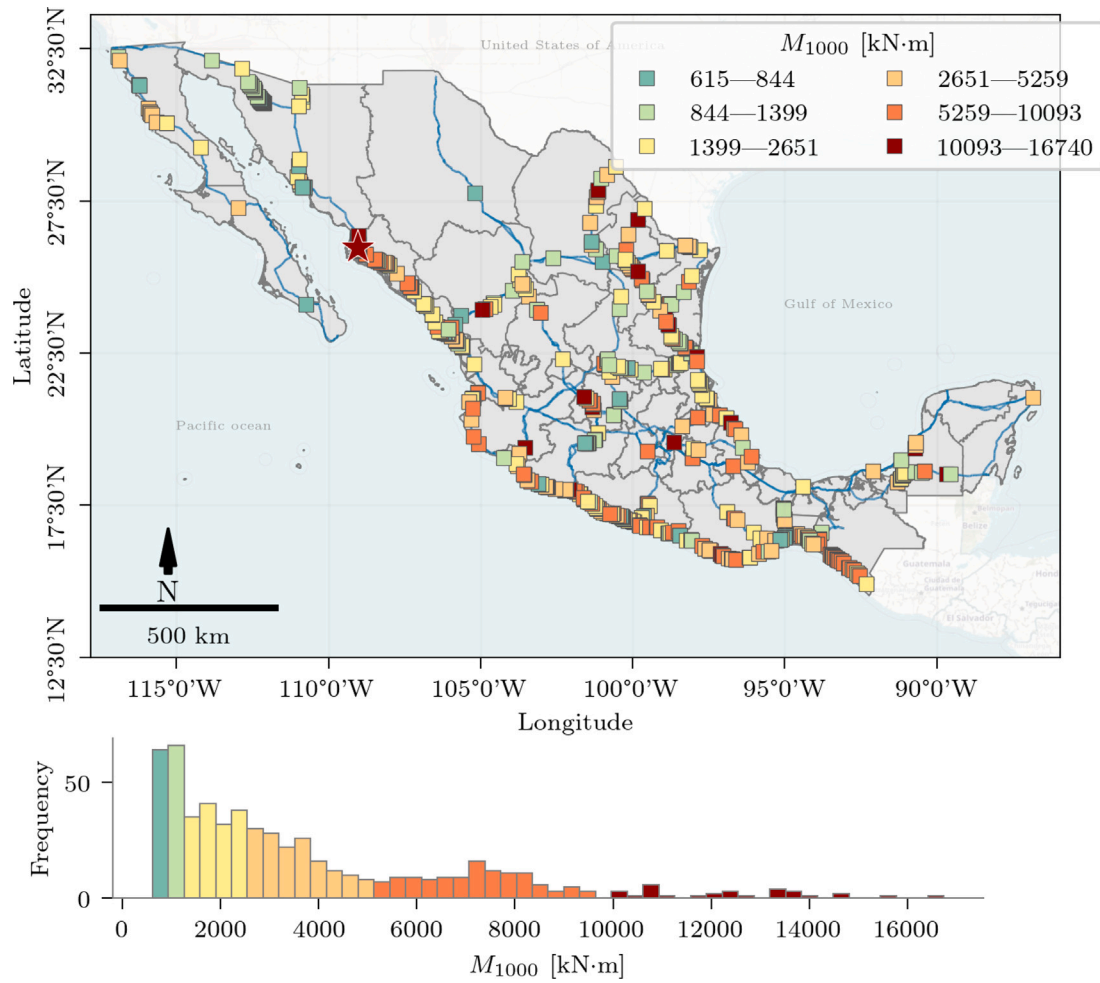


Fig. A.5. Extreme bending moments with a 1000-year return period (M_{1000}). The star marker represents the bridge with the highest M_{1000} corresponding to *Rio Fuerte* bridge with $M_{1000} = 16739.7$ kN m.

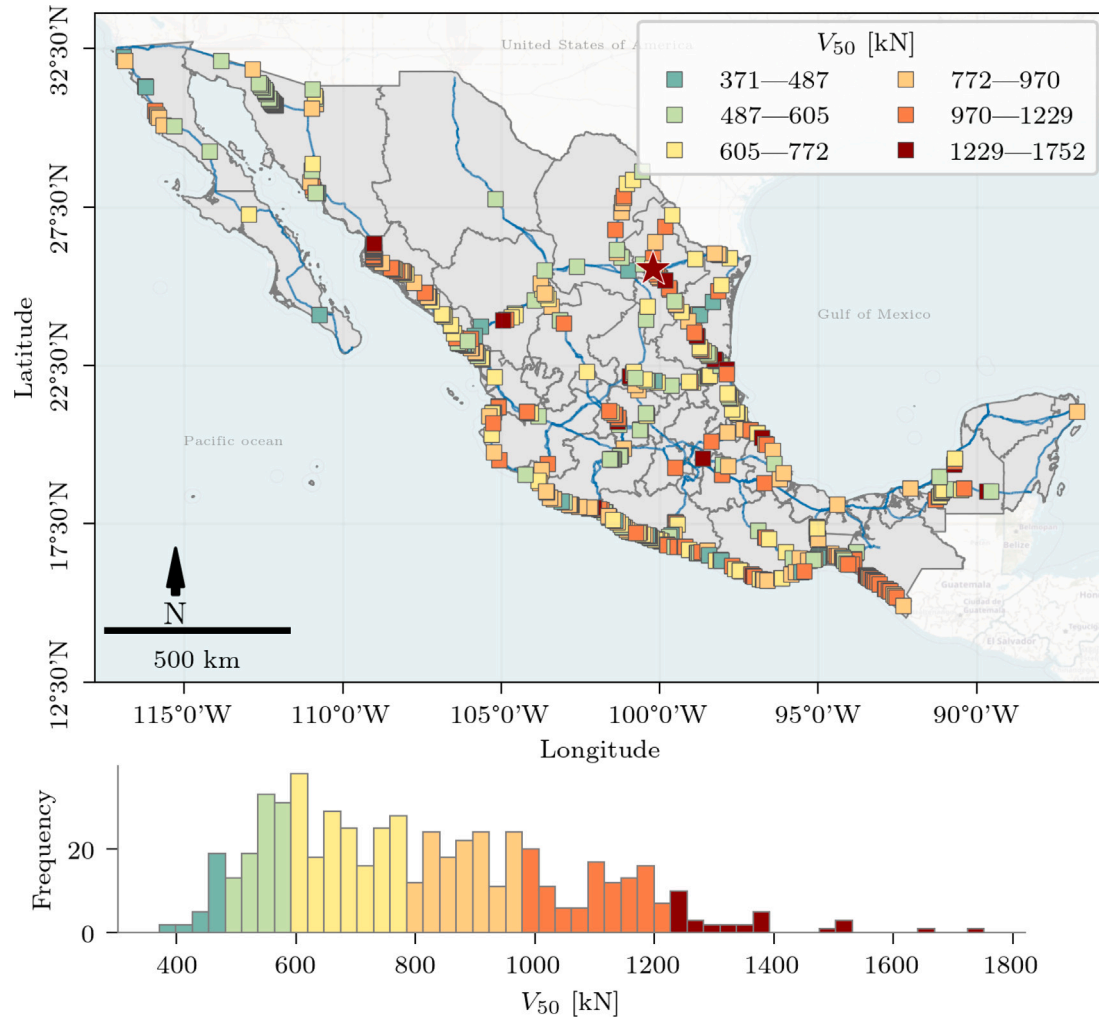


Fig. A.6. Extreme shear forces with a 50-year return period (V_{50}). The star marker represents the bridge with the highest V_{50} corresponding to *El Uro* bridge with $V_{50} = 1752.2$ kN.

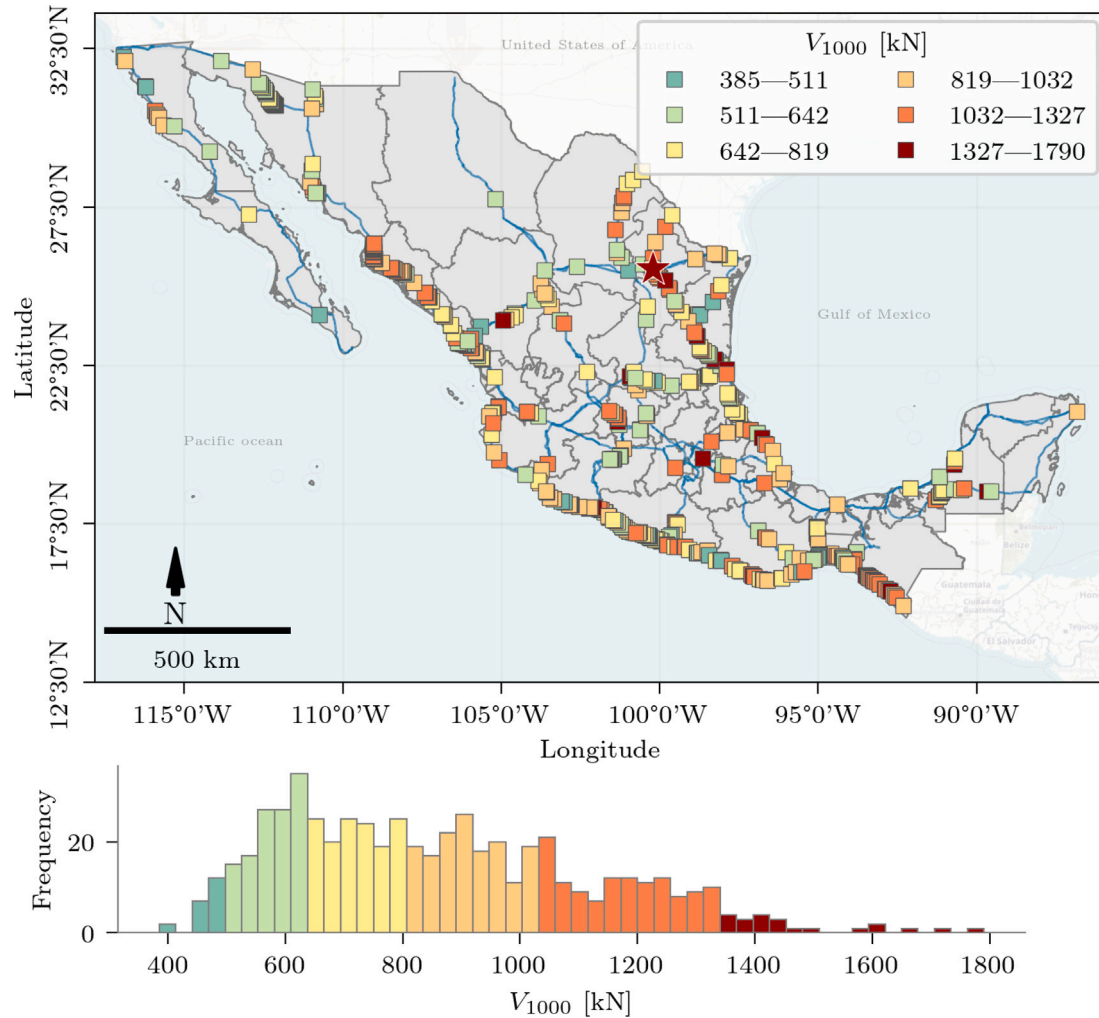


Fig. A.7. Extreme shear forces with a 1000-year return period (V_{1000}). The star marker represents the bridge with the highest V_{1000} corresponding to *El Uro* bridge with $V_{1000} = 1790.4$ kN m.

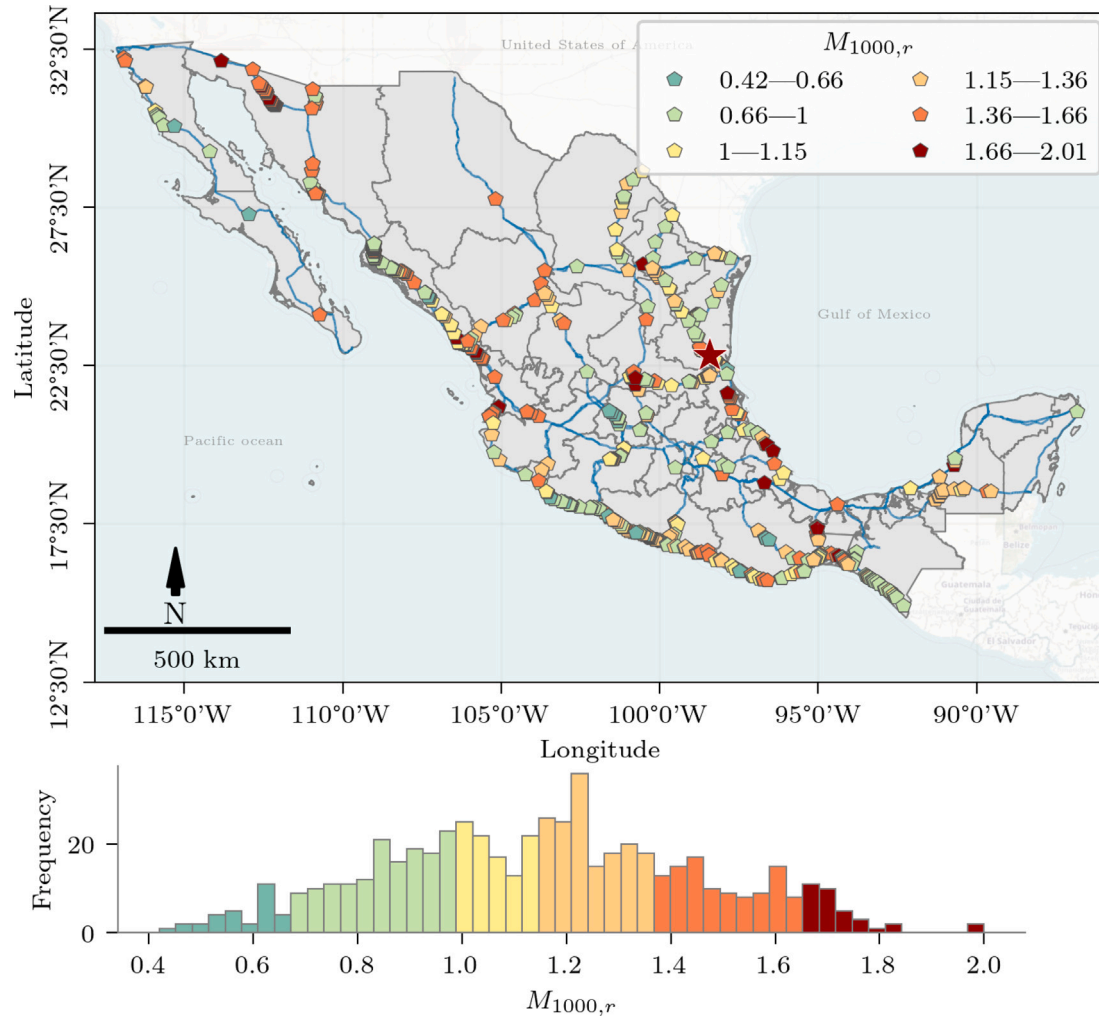


Fig. A.8. Extreme bending moment with 1000-year return period ratios ($M_{1000,r}$). Each pentagon shape marker represents a computed ratio per bridge. The star marker represents the bridge with the highest $M_{1000,r}$ corresponding to *El Cojo* bridge with $M_{1000,r} = 2$.

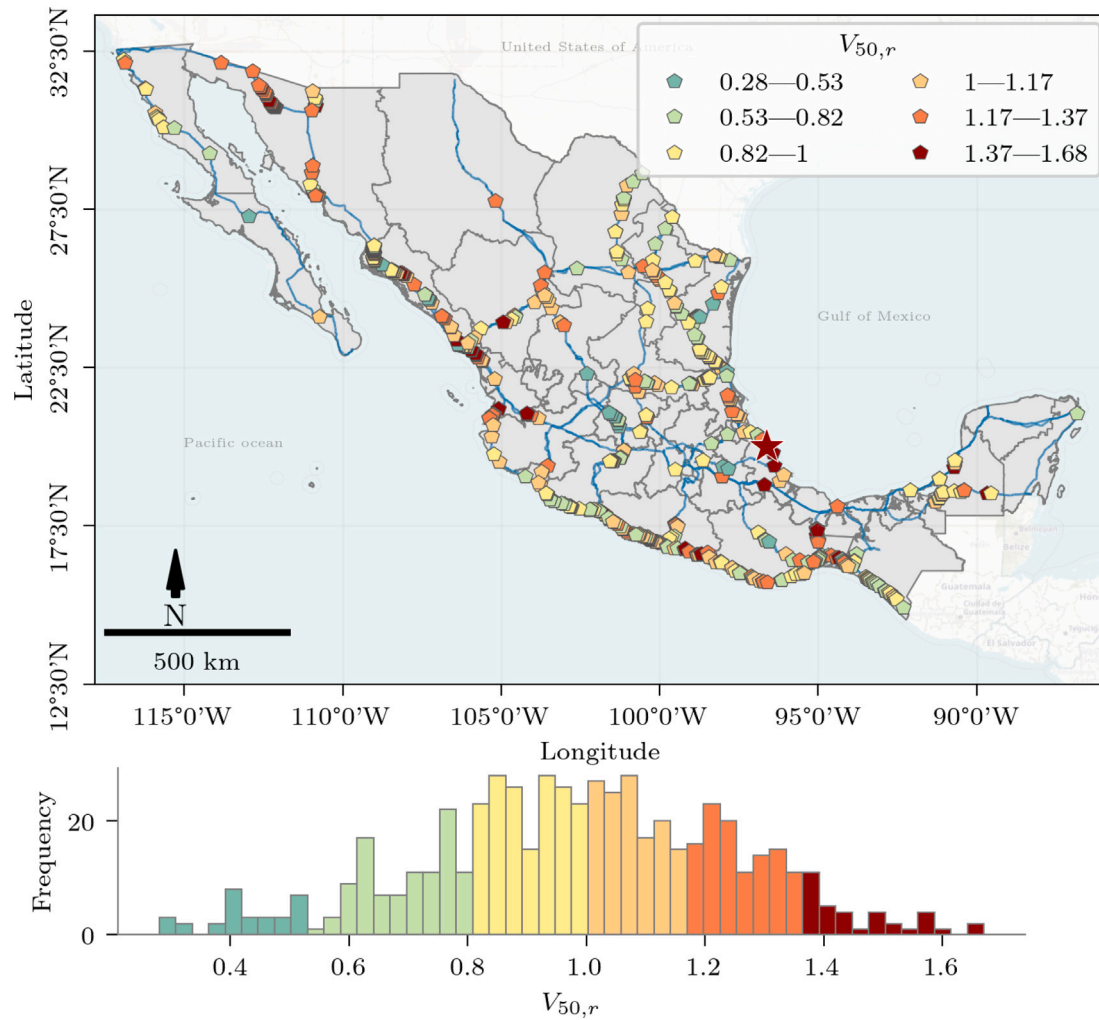


Fig. A.9. Extreme shear force with 50-year return period ratios ($V_{50,r}$). Each pentagon shape marker represents a computed ratio per bridge. The star marker represents the bridge with the highest $V_{50,r}$ corresponding to *Miraflores* bridge $V_{50,r} = 1.67$.

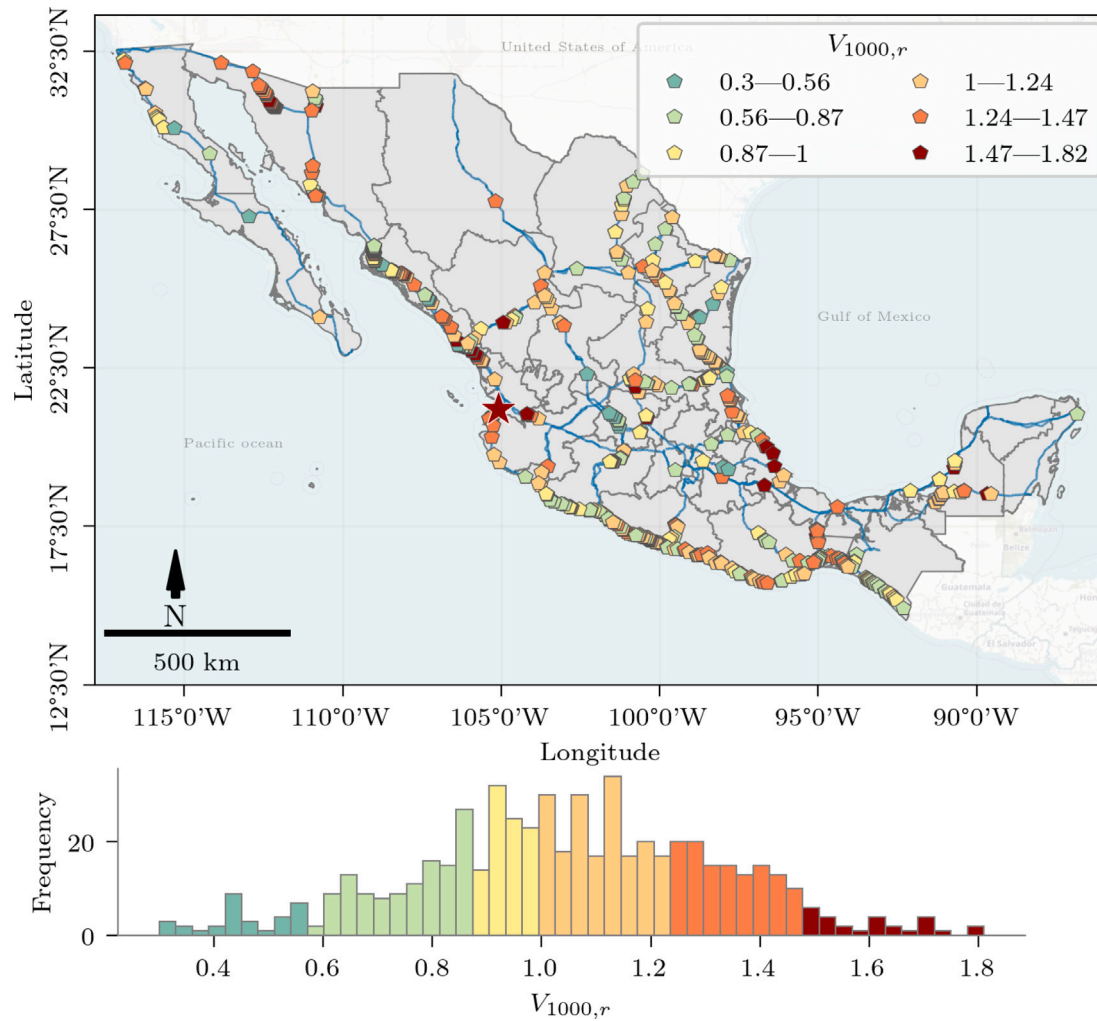


Fig. A.10. Extreme shear force with 1000-year return period ratios ($V_{1000,r}$). Each pentagon shape marker represents a computed ratio per bridge. The star marker represents the bridge with the highest $V_{1000,r}$ corresponding to *Las Piedras* bridge with $V_{50,r} = 1.81$.

Appendix B. Supplementary data

Supplementary material related to this article can be found online at <https://doi.org/10.1016/j.engstruct.2023.117172>.

References

- [1] Nogal M, O'Connor A, Caulfield B, Martinez-Pastor B. Resilience of traffic networks: From perturbation to recovery via a dynamic restricted equilibrium model. *Reliab Eng Syst Saf* 2016;156:84–96. <http://dx.doi.org/10.1016/j.res.2016.07.020>, URL <https://www.sciencedirect.com/science/article/pii/S0951832016302915>.
- [2] Pregnolato M. Bridge safety is not for granted – A novel approach to bridge management. *Eng Struct* 2019;196:109193. <http://dx.doi.org/10.1016/j.engstruct.2019.05.035>, URL <https://www.sciencedirect.com/science/article/pii/S0141029618333182>.
- [3] Farhey DN. Structural performances of bridge types in the U.S. national bridge inventory. *Infrastructures* 2018;3(1). <http://dx.doi.org/10.3390/infrastructures3010006>, URL <https://www.mdpi.com/2412-3811/3/1/6>.
- [4] Olivera CBL, Greco M, Bittencourt TN. Analysis of the Brazilian federal bridge inventory. *Rev IBRACON Estrut Mater* 2019;12(1):1–3. <http://dx.doi.org/10.1590/s1983-41952019000100002>.
- [5] COST 345 (Programme). Cost 345 : procedures required for assessing highway structures : working group 1 report on the current stock of highway structures in European countries the cost of their replacement and the annual costs of maintaining repairing and renewing them. Tech. rep., European Commission - Directorate General Research; 2003.
- [6] Ivanković AM, Skokandić D, Žnidarič A, Kreslin M. Bridge performance indicators based on traffic load monitoring. *Struct Infrastruct Eng* 2019;15(7):899–911. <http://dx.doi.org/10.1080/15732479.2017.1415941>, arXiv:<https://doi.org/10.1080/15732479.2017.1415941>.
- [7] Gonçalves MS, Lopez RH, Oroski E, Valente AM. A Bayesian algorithm with second order autoregressive errors for B-WIM weight estimation. *Eng Struct* 2022;250:113353. <http://dx.doi.org/10.1016/j.engstruct.2021.113353>, URL <https://www.sciencedirect.com/science/article/pii/S0141029621014668>.
- [8] Sjaarda M, Meystre T, Nussbaumer A, Hirt MA. A systematic approach to estimating traffic load effects on bridges using weigh-in-motion data. *Stahlbau* 2020;89(7):585–98. <http://dx.doi.org/10.1002/stab.202000048>, arXiv:<https://onlinelibrary.wiley.com/doi/pdf/10.1002/stab.202000048> URL <https://onlinelibrary.wiley.com/doi/abs/10.1002/stab.202000048>.
- [9] Maljaars J. Evaluation of traffic load models for fatigue verification of European road bridges. *Eng Struct* 2020;225:111326. <http://dx.doi.org/10.1016/j.engstruct.2020.111326>, URL <https://www.sciencedirect.com/science/article/pii/S0141029620339274>.
- [10] Martini A, Tronci EM, Feng MQ, Leung RY. A computer vision-based method for bridge model updating using displacement influence lines. *Eng Struct* 2022;259:114129. <http://dx.doi.org/10.1016/j.engstruct.2022.114129>, URL <https://www.sciencedirect.com/science/article/pii/S0141029622002656>.
- [11] Demir Ç, Dicleli M. Live load effects in hammer-head piers of continuous highway bridges and design equations based on numerical simulations verified by field tests. *Eng Struct* 2023;279:115614. <http://dx.doi.org/10.1016/j.engstruct.2023.115614>, URL <https://www.sciencedirect.com/science/article/pii/S0141029623000287>.
- [12] Hamida Z, Goulet J-A. Network-scale deterioration modelling of bridges based on visual inspections and structural attributes. *Struct Saf* 2021;88:102024. <http://dx.doi.org/10.1016/j.strusafe.2020.102024>, URL <https://www.sciencedirect.com/science/article/pii/S016747302030103X>.

- [13] Lei X, Xia Y, Dong Y, Sun L. Multi-level time-variant vulnerability assessment of deteriorating bridge networks with structural condition records. *Eng Struct* 2022;266:114581. <http://dx.doi.org/10.1016/j.engstruct.2022.114581>, URL <https://www.sciencedirect.com/science/article/pii/S0141029622006848>.
- [14] Lei X, Xia Y, Deng L, Sun L. A deep reinforcement learning framework for life-cycle maintenance planning of regional deteriorating bridges using inspection data. *Struct Multidiscip Optim* 2022;65(5):149. <http://dx.doi.org/10.1007/s00158-022-03210-3>, URL <https://doi.org/10.1007/s00158-022-03210-3>.
- [15] Lei X, Dong Y, Frangopol DM. Sustainable life-cycle maintenance policymaking for network-level deteriorating bridges with a convolutional autoencoder-structured reinforcement learning agent. *J Bridge Eng* 2023;28(9):04023063.
- [16] Lei X, Dong Y. Deep reinforcement learning for optimal life-cycle management of deteriorating regional bridges using double-deep Q-networks. *Smart Struct Syst* 2022;30(6):571–82.
- [17] Xin J, Frangopol DM, Akiyama M, Han X. Probabilistic life-cycle connectivity assessment of transportation networks using deep learning. *J Bridge Eng* 2023;28(9):04023066. <http://dx.doi.org/10.1061/JBENF2.BEENG-6149>, arXiv:<https://ascelibrary.org/doi/pdf/10.1061/JBENF2.BEENG-6149> URL <https://ascelibrary.org/doi/abs/10.1061/JBENF2.BEENG-6149>.
- [18] Lu N, Ma Y, Liu Y. Evaluating probabilistic traffic load effects on large bridges using long-term traffic monitoring data. *Sensors* 2019;19(22). <http://dx.doi.org/10.3390/s19225056>, URL <https://www.mdpi.com/1424-8220/19/22/5056>.
- [19] Yu Y, Cai C, He W, Peng H. Prediction of bridge maximum load effects under growing traffic using non-stationary bayesian method. *Eng Struct* 2019;185:171–83. <http://dx.doi.org/10.1016/j.engstruct.2019.01.085>, URL <https://www.sciencedirect.com/science/article/pii/S0141029618322089>.
- [20] Dai B, Xia Y, Li Q. An extreme value prediction method based on clustering algorithm. *Reliab Eng Syst Saf* 2022;222:108442. <http://dx.doi.org/10.1016/j.res.2022.108442>, URL <https://www.sciencedirect.com/science/article/pii/S0951832022001077>.
- [21] Jacob B. Methods for the prediction of extreme vehicular loads and load effects on bridges. *Rep Subgr* 1991;8.
- [22] Liu Y, Wang Q, Lu N. Probabilistic evaluation of maximum dynamic traffic load effects on cable-supported bridges under actual heavy traffic loads. *Proc Inst Mech Eng O: J Risk Reliab* 2021;235(1):108–19. <http://dx.doi.org/10.1177/1748006X20938491>.
- [23] Crespo-Minguillón C, Casas JR. A comprehensive traffic load model for bridge safety checking. *Struct Saf* 1997;19(4):339–59. [http://dx.doi.org/10.1016/S0167-4730\(97\)00016-7](http://dx.doi.org/10.1016/S0167-4730(97)00016-7), URL <http://www.sciencedirect.com/science/article/pii/S0167473097000167>.
- [24] Sarmadi H, Yuen K-V. Early damage detection by an innovative unsupervised learning method based on kernel null space and peak-over-threshold. *Comput-Aided Civ Infrastruct Eng* 2021;36(9):1150–67. <http://dx.doi.org/10.1111/mice.12635>, arXiv:<https://onlinelibrary.wiley.com/doi/pdf/10.1111/mice.12635> URL <https://onlinelibrary.wiley.com/doi/abs/10.1111/mice.12635>.
- [25] OBrien E, Schmidt F, Hajjalizadeh D, Zhou X-Y, Enright B, Caprani C, Wilson S, Sheils E. A review of probabilistic methods of assessment of load effects in bridges. *Struct Saf* 2015;53:44–56. <http://dx.doi.org/10.1016/j.strusafe.2015.01.002>, URL <https://www.sciencedirect.com/science/article/pii/S016747301500003X>.
- [26] Naess A, Røyset JØ. Extensions of Turkstra's rule and their application to combination of dependent load effects. *Struct Saf* 2000;22(2):129–43. [http://dx.doi.org/10.1016/S0167-4730\(00\)00004-7](http://dx.doi.org/10.1016/S0167-4730(00)00004-7), URL <https://www.sciencedirect.com/science/article/pii/S0167473000000047>.
- [27] Soriano M, Casas JR, Ghosn M. Simplified probabilistic model for maximum traffic load from weigh-in-motion data. *Struct Infrastruct Eng* 2017;13(4):454–67. <http://dx.doi.org/10.1080/15732479.2016.1164728>.
- [28] OBrien EJ, Enright B. Modeling same-direction two-lane traffic for bridge loading. *Struct Saf* 2011;33(4):296–304. <http://dx.doi.org/10.1016/j.strusafe.2011.04.004>, URL <https://www.sciencedirect.com/science/article/pii/S0167473011000427>.
- [29] OBrien E, Enright B, Dempsey T. The influence of correlation on the extreme traffic loading of bridges. In: Fifth international conference on bridge maintenance, safety and management. 2010, p. 3827–35. <http://dx.doi.org/10.1201/b10430-136>.
- [30] Jin Z, Liu W, Pei S. Probabilistic evaluation of railway vehicle's safety on bridges under random earthquake and track irregularity excitations. *Eng Struct* 2022;266:114527. <http://dx.doi.org/10.1016/j.engstruct.2022.114527>, URL <https://www.sciencedirect.com/science/article/pii/S0141029622006344>.
- [31] Arango E, Santamaria M, Nogal M, Sousa HS, Matos JC. Flood risk assessment for road infrastructures using Bayesian networks: case study of Santarem-Portugal. In: *International probabilistic workshop 2022. České vysoké učení technické v Praze*; 2022, p. 33–46.
- [32] Hong H, Huang Q, Jiang W, Tang Q, Jarrett P. Tornado wind hazard mapping and equivalent tornado design wind profile for Canada. *Struct Saf* 2021;91:102078. <http://dx.doi.org/10.1016/j.strusafe.2021.102078>, URL <https://www.sciencedirect.com/science/article/pii/S0167473021000047>.
- [33] Cignetti M, Godone D, Bertolo D, Paganone M, Thuegaz P, Giordan D. Rockfall susceptibility along the regional road network of Aosta Valley Region (north-western Italy). *J Maps* 2021;17(3):54–64. <http://dx.doi.org/10.1080/17445647.2020.1850534>.
- [34] Ma X, Zhang W, Li X, Ding Z. Evaluating tsunami damage of wood residential buildings in a coastal community considering waterborne debris from buildings. *Eng Struct* 2021;244:112761. <http://dx.doi.org/10.1016/j.engstruct.2021.112761>, URL <https://www.sciencedirect.com/science/article/pii/S0141029621009111>.
- [35] Mendoza-Lugo MA, Morales-Nápoles O, Delgado-Hernández DJ. A non-parametric Bayesian Network for multivariate probabilistic modelling of Weigh-in-Motion System Data. *Transp Res Interdiscip Perspect TA - TT -* 2022;13. <http://dx.doi.org/10.1016/j.trip.2022.100552>.
- [36] Mendoza-Lugo MA, Morales-Nápoles O. Vehicular loads hazard mapping through a Bayesian network in the state of Mexico. In: Castanier B, Cepin M, Bigaud D, Berenguer C, editors. *Proceedings of the 31st European safety and reliability conference*. Research Publishing Services; 2021, p. 2510–7. http://dx.doi.org/10.3850/978-981-18-2016-8_289-cd.
- [37] Mendoza-Lugo MA, Morales-Nápoles O. Mapping hazardous locations on a road network due to extreme gross vehicle weights. *Reliab Eng Syst Saf* 2023;109698. <http://dx.doi.org/10.1016/j.res.2023.109698>, URL <https://www.sciencedirect.com/science/article/pii/S09518320230006129>.
- [38] Koot P, Mendoza-Lugo MA, Paprotny D, Morales-Nápoles O, Ragno E, Worm DT. Pybanshee version (1.0): A python implementation of the MATLAB toolbox BAN-SHEE for non-parametric Bayesian networks with updated features. *SoftwareX* 2023;21:101279. <http://dx.doi.org/10.1016/j.softx.2022.101279>, URL <https://www.sciencedirect.com/science/article/pii/S2352711022001972>.
- [39] Blentai. PyCopula. An easy-to-use Python library that allows you to study random variables dependencies with copulas. 2019, <https://github.com/blentai/pycopula>, Last accessed: 14-09-2022.
- [40] Craig. PyNite. Simple finite element analysis in python. 2018, <https://github.com/JWock82/PyNite>, Last accessed: 14-09-2022.
- [41] Kelsey Jordahl MF, Wasserman J. Geopandas: v0.8.1. 2020, <http://dx.doi.org/10.5281/zenodo.3946761>.
- [42] QGIS Development Team. QGIS Geographic Information System. QGIS Association; 2022, URL <https://www.qgis.org>.
- [43] Dirección General de Conservación de Carreteras. Puentes de la red federal de carreteras. Sistema de puentes de México (SIPUMEX). 2021, <https://www.sct.gob.mx/carreteras/direccion-general-de-conservacion-de-carreteras/puentes-de-la-red-federal-de-carreteras/>, Last accessed: 29-01-2023.
- [44] Secretaría de Comunicaciones y Transporte. N-pry-car-6-01-001, ejecución de proyectos de nuevos puentes y estructuras similares. 2001, p. 14, URL <https://normas.imt.mx/normativa/N-PRY-CAR-6-01-001-01.pdf>.
- [45] American Association of State Highway and Transportation Officials. Standard specifications for highway bridges. Aashto; 2002.
- [46] García-Soto A, Hernández-Martínez A, Valdés-Vázquez J. Probabilistic assessment of a design truck model and live load factor from weigh-in-motion data for Mexican highway bridge design. *Can J Civil Eng* 2015;42(11):970–4. <http://dx.doi.org/10.1139/cjce-2015-0216>, arXiv:<https://doi.org/10.1139/cjce-2015-0216>.
- [47] Hernández JLG, González NG. Análisis estadístico para la generación de información proveniente de estaciones dinámicas de medición de pesos, dimensiones y velocidades vehiculares para 2019. *Tech. rep, SCT*; 2021.
- [48] Dirección General de Servicios Técnicos. Datos viales 2021. 2021, <https://www.sct.gob.mx/carreteras/direccion-general-de-servicios-tecnicos/datos-viales/2021/>, Last accessed: 29-01-2023.
- [49] Instituto Mexicano del Transporte. Consulta de la base de datos del EECAN. 2022, <https://www.imt.mx/micrositios/seguridad-y-operacion-del-transporte/estadisticas/consulta-del-eeacan.html>, Last accessed: 29-01-2023.
- [50] Nowak M, Fischer O. Realistic traffic-data based load models for existing road bridges. In: *IABSE Congress: Challenges in Design and Construction of an Innovative and Sustainable Built Environment*. 2016, p. 21–3. <http://dx.doi.org/10.2749/stockholm.2016.0239>, Stockholm, Sweden, 21-23 September 2016.
- [51] Hernández Gutiérrez JL, Soria Anguiano V, Dorado Pineda ML. Estudio estadístico de campo del autotransporte nacional: análisis estadístico de la información recopilada en las estaciones instaladas en 2017. *Tech. rep. 75, SCT*; 2018.
- [52] SCT. NOM-012-SCT-2-2017, sobre el peso y dimensiones máximas con los que pueden circular los vehículos de autotransporte que transitan en las vías generales de comunicación de jurisdicción federal. 2017, p. 36.
- [53] Federal Highway Administration's Intelligent Transportation Systems Program Office. A summary of vehicle detection and surveillance technologies used in intelligent transportation systems. *Tech. rep., New Mexico State University*; 2007.
- [54] Srinivas S, Devdas M, Prasad AM. Multivariate simulation and multi-modal dependence modeling of vehicle axle weights with copulas. *J Transp Eng* 2006;132(12):945–55. [http://dx.doi.org/10.1061/\(ASCE\)0733-947X\(2006\)132:12\(945\)](http://dx.doi.org/10.1061/(ASCE)0733-947X(2006)132:12(945)).
- [55] Oswald M-N, M. SRDJ. Large-scale hybrid Bayesian network for traffic load modeling from weigh-in-motion system data. *J Bridge Eng* 2015;20(1):4014059. [http://dx.doi.org/10.1061/\(ASCE\)BE.1943-5592.0000636](http://dx.doi.org/10.1061/(ASCE)BE.1943-5592.0000636).
- [56] And DA, Vervuurt OMNA. Traffic load model for short span bridges. *Tech. rep., Delft: Nederlandse Organisatie voor Toegepast Natuurwetenschappelijk Onderzoek*; 2015.

- [57] Morales-Nápoles O, Steenbergen RD. Analysis of axle and vehicle load properties through Bayesian networks based on weigh-in-motion data. *Reliab Eng Syst Saf* 2014;125:153–64. <http://dx.doi.org/10.1016/j.res.2014.01.018>, URL <https://www.sciencedirect.com/science/article/pii/S0951832014000283>, Special issue of selected articles from ESREL 2012.
- [58] Torres-Alves G, 't Hart C, Morales-Nápoles O, Jonkman S. Structural reliability analysis of a submerged floating tunnel under copula-based traffic load simulations. *Eng Struct* 2022;269:114752. <http://dx.doi.org/10.1016/j.engstruct.2022.114752>, URL <https://www.sciencedirect.com/science/article/pii/S0141029622008409>.
- [59] Calvert G, Neves L, Andrews J, Hamer M. Modelling interactions between multiple bridge deterioration mechanisms. *Eng Struct* 2020;221:111059. <http://dx.doi.org/10.1016/j.engstruct.2020.111059>, URL <https://www.sciencedirect.com/science/article/pii/S0141029619347637>.
- [60] Mendoza-Lugo MA, Delgado-Hernández DJ, Morales-Nápoles O. Reliability analysis of reinforced concrete vehicle bridges columns using non-parametric Bayesian networks. *Eng Struct* 2019;188:178–87. <http://dx.doi.org/10.1016/j.engstruct.2019.03.011>, URL <https://www.sciencedirect.com/science/article/pii/S014102961833565X>.
- [61] Vervuurt A, Pruiksmá J, Steenbergen R, Courage W, Miraglia S, Morales Nápoles O. Statische belastingen Herijking verkeersbelastingen voor brugconstructies op basis van WIM analyses van april 2013, Vol. Droge kunstwerken. TNO-2014-R11653, *InfraQuest*; 2015.
- [62] Kosgodagan-Dalla Torre A, Yeung TG, Morales-Nápoles O, Castanier B, Maljaars J, Courage W. A two-dimension dynamic Bayesian network for large-scale degradation modeling with an application to a bridges network. *Comput-Aided Civ Infrastruct Eng* 2017;32(8):641–56. <http://dx.doi.org/10.1111/mice.12286>, arXiv:<https://onlinelibrary.wiley.com/doi/pdf/10.1111/mice.12286> URL <https://onlinelibrary.wiley.com/doi/abs/10.1111/mice.12286>.
- [63] Rascon Chavez O, Brussee Moreno M, Ventura Suarez G. Análisis normativo y estadístico de cargas vivas en puentes en México. *Publ Téc* 1997;32(97).
- [64] Federal Highway Administration. Bridge formula weights. 2023, https://ops.fhwa.dot.gov/freight/publications/brdg_fm_wghts/, Accessed: May 30, 2023.
- [65] Guo D, Caprani CC. Traffic load patterning on long span bridges: A rational approach. *Struct Saf* 2019;77:18–29. <http://dx.doi.org/10.1016/j.strusafe.2018.11.003>, URL <https://www.sciencedirect.com/science/article/pii/S0167473018300304>.
- [66] Treiber M, Hennecke A, Helbing D. Microscopic simulation of congested traffic. In: Helbing D, Herrmann HJ, Schreckenberg M, Wolf DE, editors. *Traffic and granular flow '99*. Berlin, Heidelberg: Springer Berlin Heidelberg; 2000, p. 365–76.
- [67] Carey C, Caprani CC, Enright B. A pseudo-microsimulation approach for modelling congested traffic loading on long-span bridges. *Struct Infrastruct Eng* 2018;14(2):163–76. <http://dx.doi.org/10.1080/15732479.2017.1330893>, arXiv:<https://doi.org/10.1080/15732479.2017.1330893>.
- [68] Ge L, Dan D, Liu Z, Ruan X. Intelligent simulation method of bridge traffic flow load combining machine vision and weigh-in-motion monitoring. *IEEE Trans Intell Transp Syst* 2022;23(9):15313–28. <http://dx.doi.org/10.1109/TITS.2022.3140276>.
- [69] Dan D, Xu Z, Zhang K, Yan X. Monitoring index of transverse collaborative working performance of assembled beam bridges based on transverse modal shape. *Int J Struct Stab Dyn* 2019;19. <http://dx.doi.org/10.1142/S021945541950086X>.
- [70] Caprani CC, OBrien EJ, Lipari A. Long-span bridge traffic loading based on multi-lane traffic micro-simulation. *Eng Struct* 2016;115:207–19. <http://dx.doi.org/10.1016/j.engstruct.2016.01.045>, URL <https://www.sciencedirect.com/science/article/pii/S0141029616000614>.
- [71] Yang DY, Frangopol DM. Life-cycle management of deteriorating bridge networks with network-level risk bounds and system reliability analysis. *Struct Saf* 2020;83:101911. <http://dx.doi.org/10.1016/j.strusafe.2019.101911>, URL <https://www.sciencedirect.com/science/article/pii/S0167473019303753>.
- [72] Sklar M. *Fonctions de répartition à n dimensions et leurs marges*. Université Paris 8; 1959.
- [73] Joe H. *Dependence modeling with copulas*. CRC Press; 2014.
- [74] Neath AA, Cavanaugh JE. The Bayesian information criterion: background, derivation, and applications. *WIREs Comput Stat* 2012;4(2):199–203. <http://dx.doi.org/10.1002/wics.199>, arXiv:<https://wires.onlinelibrary.wiley.com/doi/pdf/10.1002/wics.199> URL <https://wires.onlinelibrary.wiley.com/doi/abs/10.1002/wics.199>
- [75] Szmídt E, Kacprzyk J. The spearman rank correlation coefficient between intuitionistic fuzzy sets. In: *2010 5th IEEE international conference intelligent systems*. IEEE; 2010, p. 276–80.
- [76] Fiorillo G, Ghosn M. Application of influence lines for the ultimate capacity of beams under moving loads. *Eng Struct* 2015;103:125–33. <http://dx.doi.org/10.1016/j.engstruct.2015.09.003>, URL <https://www.sciencedirect.com/science/article/pii/S0141029615005660>.
- [77] Fußeder M, Wüchener R, Bletzinger K-U. Towards a computational engineering tool for structural sensitivity analysis based on the method of influence functions. *Eng Struct* 2022;265:114402. <http://dx.doi.org/10.1016/j.engstruct.2022.114402>, URL <https://www.sciencedirect.com/science/article/pii/S0141029622005168>.
- [78] OBrien EJ, Cantero D, Enright B, González A. Characteristic dynamic increment for extreme traffic loading events on short and medium span highway bridges. *Eng Struct* 2010;32(12):3827–35. <http://dx.doi.org/10.1016/j.engstruct.2010.08.018>, URL <https://www.sciencedirect.com/science/article/pii/S014102961000307X>.
- [79] Bailey SF. *Basic principles and load models for the structural safety evaluation of existing road bridges*. Tech. rep., EPFL; 1996.
- [80] O'connor A, O'Brien EJ. Traffic load modelling and factors influencing the accuracy of predicted extremes. *Can J Civil Eng* 2005;32(1):270–8.
- [81] Caprani CC. *Probabilistic analysis of highway bridge traffic loading* (Ph.D. thesis), Technological University Dublin; 2005.
- [82] Martucci D, Civera M, Surace C. Bridge monitoring: Application of the extreme function theory for damage detection on the I-40 case study. *Eng Struct* 2023;279:115573. <http://dx.doi.org/10.1016/j.engstruct.2022.115573>, URL <https://www.sciencedirect.com/science/article/pii/S0141029622016492>.
- [83] Castillo E, O'Connor AJ, Nogal M, Calviño A. On the physical and probabilistic consistency of some engineering random models. *Struct Saf* 2014;51:1–12. <http://dx.doi.org/10.1016/j.strusafe.2014.05.003>, URL <https://www.sciencedirect.com/science/article/pii/S016747301400054X>.
- [84] Kwak M. Genome-wide association study using truncated likelihood with incomplete information for stratum specific missingness. *J Korean Stat Soc* 2021;50(1):117–33. <http://dx.doi.org/10.1007/s42952-020-00064-7>.
- [85] Morales-Nápoles O, Steenbergen RD. Analysis of axle and vehicle load properties through Bayesian Networks based on Weigh-in-Motion data. *Reliab Eng Syst Saf* 2014;125:153–64. <http://dx.doi.org/10.1016/j.res.2014.01.018>.
- [86] Steenbergen R, Nápoles OM, Vrouwenvelder A. *Algemene veiligheidsbeschouwing en modellering van wegverkeerbelasting voor brugconstructies*. Update van TNO rapport 98-CON-R1813. Tech. rep., TNO; 2012.
- [87] Caprani CC, Belay A, O'Connor A. Site-specific probabilistic load modelling for bridge reliability analysis. In: *Proceedings of the 3rd. international conference on current and future trends in bridge design, construction and maintenance*. 2003, p. 341–8.
- [88] O'Connor AJ. *Probabilistic traffic load modelling for highway bridges* (Ph.D. thesis), Trinity College Dublin; 2001.
- [89] Leahy C, OBrien E, O'Connor A. The effect of traffic growth on characteristic bridge load effects. *Transp Res Procedia* 2016;14:3990–9. <http://dx.doi.org/10.1016/j.trpro.2016.05.496>, URL <https://www.sciencedirect.com/science/article/pii/S2352146516305038>, Transport Research Arena TRA2016.
- [90] OBrien E, Bordallo-Ruiz A, Enright B. Lifetime maximum load effects on short-span bridges subject to growing traffic volumes. *Struct Saf* 2014;50:113–22. <http://dx.doi.org/10.1016/j.strusafe.2014.05.005>, URL <https://www.sciencedirect.com/science/article/pii/S0167473014000563>.
- [91] Meng Z, Zhao J, Jiang C. An efficient semi-analytical extreme value method for time-variant reliability analysis. *Struct Multidiscip Optim* 2021;64(3):1469–80. <http://dx.doi.org/10.1007/s00158-021-02934-y>.
- [92] Secretaría de Comunicaciones y Transporte. N-pry-car-6-01-003, *cargas y acciones*. 2001, p. 25.
- [93] European Committee S. EN 1991-2:2003 eurocode 1: Actions on structures - part 2: Traffic loads on bridges. 2003.
- [94] Diario Oficial de la Federación. ACUERDO SS/3/2022 por el que se determina el calendario oficial de suspensión de labores para el año 2022. 2022.
- [95] Mutua FM. The use of the Akaike Information Criterion in the identification of an optimum flood frequency model. *Hydrol Sci J* 1994;39(3):235–44. <http://dx.doi.org/10.1080/02626669409492740>, arXiv:<https://doi.org/10.1080/02626669409492740>.
- [96] Delft High Performance Computing Centre (DHPC). *Delftblue supercomputer (Phase 1)*. 2022, <https://www.tudelft.nl/dhpc/ark:/44463/DelftBluePhase1>.
- [97] Getachew A, OBrien EJ. Simplified site-specific traffic load models for bridge assessment. *Struct Infrastruct Eng* 2007;3(4):303–11. <http://dx.doi.org/10.1080/15732470500424245>, arXiv:<https://doi.org/10.1080/15732470500424245>.
- [98] Chávez O, Instituto Mexicano del Transporte. *Análisis normativo y estadístico de cargas vivas en puentes en México*. Publicación técnica, Instituto Mexicano del Transporte, Secretaría de Comunicaciones y Transportes; 1997.
- [99] Chávez O, Instituto Mexicano del Transporte. *Modelo de cargas vivas vehiculares para diseño estructural de puentes en México*. Publicación técnica, Instituto Mexicano del Transporte, Secretaría de Comunicaciones y Transportes; 1999.